

## **SOUTHERN CALIFORNIA PARTICLE SUPERSITE**

### **Progress Report for Period July 1, 2002 – October 1, 2002**

#### **United States Environmental Protection Agency**

**Principal Investigator:** John R. Froines, Ph.D., UCLA School of Public Health

**Co-Principal Investigator:** Constantinos Sioutas, Sc.D., USC School of Engineering

### **1. Introduction**

The overall objective of the Southern California Particle Supersite is to conduct research and monitoring that contributes to a better understanding of the measurement, sources, size distribution, chemical composition and physical state, spatial and temporal variability, and health effects of suspended particulate matter (PM) in the Los Angeles Basin (LAB). This report addresses the period from July 1, 2002 through October 1, 2002. It is divided into 10 sections, each addressing a specific research area, including an update on our Data Management report. Furthermore, a major portion of the information included in this report has been either submitted or accepted for publication in peer-reviewed journals. Below is a list of manuscripts either submitted or accepted for publication which were produced through the Southern California Supersite funds and in which the EPA Supersite program has been acknowledged.

### **2. List of Publications:**

1. Singh, M., Jaques, P. and Sioutas, C. "Particle-bound metals in source and receptor sites of the Los Angeles Basin". *Atmospheric Environment*, 36(10): 1675-168, 2002 .
2. Kim, S., Shi, S., Zhu, Y., Hinds, W.C., and Sioutas, C. "Size Distribution, Diurnal and Seasonal Trends of Ultrafine Particles in Source and Receptor Sites of the Los Angeles Basin". *Journal of Air and Waste Management Association*, 52:174-185, 2002
3. Li, N., Kim, S., Wang, M., Froines, J.R., Sioutas, C. and Nel, A. "Use of a Stratified Oxidative Stress Model to Study the Biological Effects of Ambient Concentrated and Diesel Exhaust Particulate Matter". *Inhalation Toxicology*, 14(5): 459-486, 2002
4. Zhu, Y., Hinds, W.C., Kim, S., Shen, S. and Sioutas, C. "Study on Ultrafine Particles and other Vehicular Pollutants near a Busy Highway Dominated by Diesel Traffic". *Atmospheric Environment*. 36, 4375-4383, 2002
5. Eiguren, A, Miguel, A.H, Jaques, P. and Sioutas, C. "Evaluation of a Denuder-MOUDI-PUF Sampling System to Determine the Size Distribution of Semivolatile Polycyclic

Aromatic Hydrocarbons in the Atmosphere”. Manuscript accepted for publication in *Aerosol Science and Technology*, June 2002.

6. Zhu, Y., Hinds, W.C., Kim, S and Sioutas, C. “Concentration and Size Distribution of Ultrafine Particles near a Major Highway”. *Journal of Air and Waste Management Association*, 52:1032-1042, 2002
7. Geller, M.D., Kim, S. Misra, C., Sioutas, C., Olson, B.A and Marple, V.A. “Methodology for measuring size-dependent chemical composition of ultrafine particles “ *Aerosol Science and Technology*, 36(6): 748-763, 2002
8. Misra, C., Kim S., Shen S. and Sioutas C. “Design and evaluation of a high-flow rate, very low pressure drop impactor for separation and collection of fine from ultrafine particles”. *Journal of Aerosol Science*, 33(5): 735-752, 2002
10. Fine, P.M., Hering, S.V., Jaques P.A. and Sioutas, C. “Performance Evaluation and Field Use of a Continuous Monitor for Measuring Size-Segregated PM<sub>2.5</sub> Particulate Nitrate”. Manuscript submitted to *Aerosol Science and Technology*, March 2002
11. Misra, C., Geller, M.D., Solomon, P.A. and Sioutas, C. “Development of a PM<sub>10</sub> Inertial Impactor for Coarse Particle Measurement and Speciation.” *Aerosol Science and Technology*, in press, August 2002
12. Stolzenburg, M.R., Dutcher, D., Kirby, B., Kreisberg, N. and Hering, S.V. (2002). Automated Measurement of the Size Distribution of Airborne Particulate Nitrate. Submitted to *Aerosol Science & Technology*, April 002
13. Shen, S., Zhu, Y., Jaques PA and Sioutas C. “Evaluation of the SMPS-APS system as a Continuous Monitor for PM<sub>2.5</sub> and PM<sub>10</sub>”. *Atmospheric Environment*, in press , 2002
14. Emma Di Stefano Yoshito Kumagai, Antonio H. Miguel, Arantzazu Eiguren, Takahiro Kobayashi, Ed Avol and John R. Froines “Determination of four Quinones/Hydroquinones in Diesel Exhaust Particles and Atmospheric PM<sub>2.5</sub>” Submitted to *Aerosol Science and Technology*, October 2002
15. Philip M. Fine, Si Shen, Michael Geller and Constantinos Sioutas “Inferring the sources of PM<sub>2.5</sub> at downwind receptor sites in the Los Angeles Basin using multiple semi-continuous monitors “Submitted to *Aerosol Science and Technology*, October 2002
16. Jeff Ambs, Peter Jaques and Constantinos Sioutas “Field Evaluation Of The Differential TEOM® Monitor By Comparison With Semi-continuous And Integrated Ambient Particulate Mass And Nitrate In Claremont, California” Submitted to *Aerosol Science and Technology*, October 2002

17. Bhabesh Chakrabarti, Manisha Singh and Constantinos Sioutas “Development of a Near-Continuous Monitor for Measurement of the Ultrafine PM Mass Concentration” Submitted to *Aerosol Science and Technology*, October 2002
18. Yifang Zhu, , William C. Hinds, Si Shen, and Constantinos Sioutas “Seasonal Trends of Concentration and Size Distributions of Ultrafine Particles Near Major Freeways in Los Angeles”. Submitted to *Aerosol Science and Technology*, October 2002

### 3. PIU Sampling Location and Status

A key feature of our Supersite activities has been in the ability to conduct state-of the art measurements of the physiochemical characteristic of PM in different locations of the Los Angeles basin (LAB). We originally proposed a 2.5-year repeating cycle of measurements at five locations. Each location will be sampled during a period of intense photo-chemistry (defined approximately as May-October) and low photochemical activity (defined as the period between November-April). During the period of this progress report, PM sampling with the Particle Instrumentation Unit (PIU) at Claremont, the fourth Southern California Supersite location, has been completed. The full term of sample collection was between September 2001 and August 2002. We have completed all chemical speciation analysis for integrated samples, except for the following: 1) Metals, June, July, and early August expected to be completed for the next report; 2) EC/OC, July and August analysis is near completion. We have continued to make size integrated on-line measurements of particulate nitrate and carbon using the Integrated Collection and Vaporization System (ICVS) developed by Aerosol Dynamics Inc. A continuous BAM monitor was installed and has been paired with the USC-TEOM coarse monitor to generate hourly data of coarse, fine, and ultrafine PM. Additionally, we have continued to make our mobile particle trailer available for co-located exposure studies at Claremont, and have arranged to participate in further studies in the next location at USC.

The trailer has been moved from Claremont to the fifth Supersite location on the USC campus during the third week in September 2002. The USC campus is about 1-2 miles of two major freeways, and about 3-5 miles south of downtown Los Angeles.

The following health studies have been supported by the Supersite measurements: In vitro studies undertaken by Drs. Andre Nel and Arthur Cho (UCLA) investigating the hypotheses that organic constituents associated with PM, including quinines, other organic compounds (PAHs, nitro-PAHs, and aldehydes/ketones) and metals are capable of generating reactive oxygen species (ROS) and acting as electrophilic agents. These are ongoing studies. Animal inhalation toxicology studies using Concentrated Ambient Particulates (CAP) investigating the hypotheses that atmospheric chemistry is important in the toxicity of PM and co-pollutants, airway injury and cardiovascular effects will be greater at receptor sites downwind of source sites along the mobile source trajectory in the Los Angeles basin. Led by Drs. Harkema (University of

Michigan), Kleinman (UC Irvine), Froines, and Nel (UCLA), these co-located studies that commenced during the summer season 2001 in Claremont continued through this past winter to investigate seasonal changes in toxicity, and is currently being set up USC for a early Fall exposure study.

#### **4. Time Integrated Size Fractioned Chemical Speciation for Claremont**

##### **Introduction**

Our current sampling scheme continues to involve the use of three MOUDIs for 24-hour averages: size-fractionated measurements of ambient and concentrated PM mass and chemical composition. Additionally, a Partisol is used to acquire the coarse fraction of mass. Sampling is conducted once a week, on a Tuesday, Wednesday or Thursday, in order to coincide with one of the sampling days of the AQMD speciation network (which takes place every 3<sup>rd</sup> day). However, this schedule is flexible to be adjusted for our “intensive” particulate characterization studies and/or for our support of co-located health effects exposure studies. Typically, ambient data are averaged over 24 hours (midnight to midnight), whereas for exposure or source contribution measurements, the time integrals may vary. In each run, consistent with our original Supersite proposal, we have used three collocated Micro-Orifice Uniform Deposit Impactors (MOUDI) to generate five PM size ranges:

<0.1 $\mu\text{m}$	(ultrafine particles)
0.1- 0.32 $\mu\text{m}$	(accumulation mode, “condensation” sub-mode)
0.32 – 1.0 $\mu\text{m}$	(accumulation mode, “droplet” sub-mode)
1.0 – 2.5	(“intermediate” mode)
2.5-10 $\mu\text{m}$	(coarse particles)

In addition to mass concentration, the following chemical components have been analyzed within these size groups: inorganic ions (i.e., sulfate, nitrate, ammonium), analyzed by ion chromatography (Dionex); trace elements and metals, analyzed by XRF; and the elemental and organic carbon (EC/OC) content is analyzed by thermal optical detection. Data collection is complete through August 21 for mass, August 6 for ions, June 25 for EC/OC, and June 5 for Metals. Thus, the metal data is the same as in the previous report, and the ion and EC/OC data is updated between 4 and 8 weeks, but only the mass is complete for the full term of measurements made at Claremont. A final summary of the full mass and chemical balance will be included in the next report.

##### **Results**

Figure 1 presents the size distribution of particle mass measured by the MOUDI for PM less than 2.5  $\mu\text{m}$ , and by the Partisol for the coarse mode. Fine PM (19.7  $\mu\text{g}/\text{m}^3$ ) is barely less than Coarse (20.2 $\mu\text{g}/\text{m}^3$ ), a slight shift from the previous report where PM<sub>2.5</sub> was at 18.9, and the Coarse at 16.3 $\mu\text{g}/\text{m}^3$ . Since the full chemical analysis is not yet available, we are not prepared to

discuss the chemical group that predominantly contributes to this increase, although as seen in the following figures, albeit lacking summer data, it's likely dominated by Metal Oxides. In the Fine fraction, as per the spring report, PM mass continues to predominate in the accumulation "droplet" sub-mode (8.9 ug/m<sup>3</sup>), suggesting aged particles. The Ultrafine mode consists of the lowest mass at 1.0 ug/m<sup>3</sup>.

Figure 2 presents a paired time series plot of coarse and fine PM for the full term at Claremont (September 2001 to August 2002). Coarse values range from 0.27 ug/m<sup>3</sup> in late November 2001 to 39.9 ug/m<sup>3</sup> in early June. Typically, the warmer (i.e., Summer) months were highest for Coarse particles. Fine PM followed a similar seasonal pattern, ranging from 3 ug/m<sup>3</sup> in late November to 48 ug/m<sup>3</sup> in the warmer period. For the most part, both fractions tracked a similar pattern, with either predominating on any given day. Since the coarse fraction is influenced by wind, and the fine fraction is dominated by the accumulation mode, this suggests that for most occasions (i.e., where the Fine and Coarse fractions track each other) that the Fine fraction is transported rather than from local source emissions.

Size speciated mass measurements are presented in Figures 3 – 6 and Table 1. Figure 3 and 4 show that the coarse fraction is dominated by Metal Oxides, likely from local re-suspended road dust. The Fine fraction is dominated by Ammonium Nitrate, which predominates in the droplet (2.7 ug/m<sup>3</sup>), and secondly in the intermediate mode (2.5 ug/m<sup>3</sup>). Claremont is a receptor site North West of the dairy farms, and diurnally receives winds from this direction, possibly contributing to the relatively high Ammonium Nitrate in the larger modes of the fine PM fraction. Organic Carbon is higher in PM<sub>2.5</sub> than coarse, and highest in the Accumulation Mode (3.3 ug/m<sup>3</sup>). It is in greatest relative concentration in the droplet mode (1.78 ug/m<sup>3</sup>). Since Claremont is a "freeway" trajectory site, it may be expected that aged enlarged OC-associated particulate matter predominate. Compared to other groups of the Fine fraction, Ammonium Nitrate is greatest in the intermediate mode, while Organic Carbon is equally for the ultrafine fraction.

Figure 5 presents a comparison of the size speciated total filter mass to that of the summed chemical species described above. Figure 6 presents a ratio of the two by size fraction. Except for the Ultrafine mode (2.4) and Coarse mode (66%), the sum of the measured chemical groups explains between 77 to 86% of the total measured particulate mass for the other modes. This is slightly inaccurate, as the total chemical mass database is slightly incomplete. As noted above, the coarse fraction increased a few percent, and this may be due to Metals, of which data is not yet in. Also, since the ultrafine filter mass is less than 5% of the total filter mass, the relative chemical mass is not as reliable a measurement.

Figure 1. Size distribution of particle mass measured by MOUDI (< 2.5  $\mu\text{m}$ ) and Partisol (10 - 2.5  $\mu\text{m}$ ).

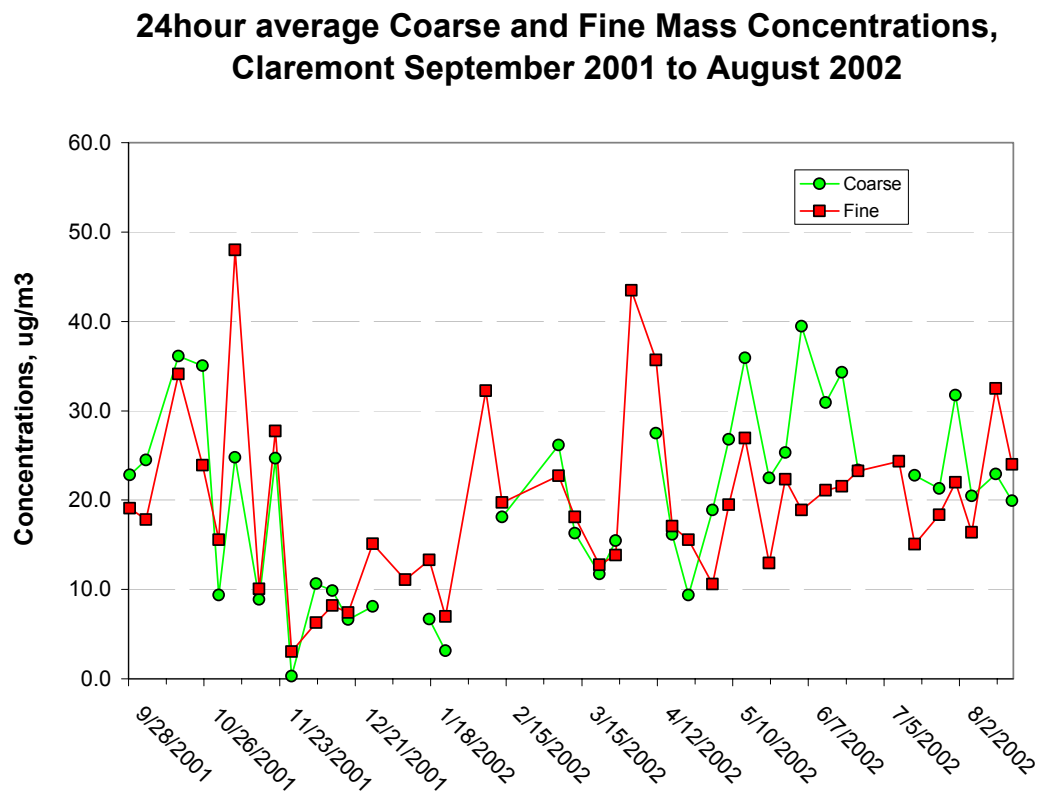
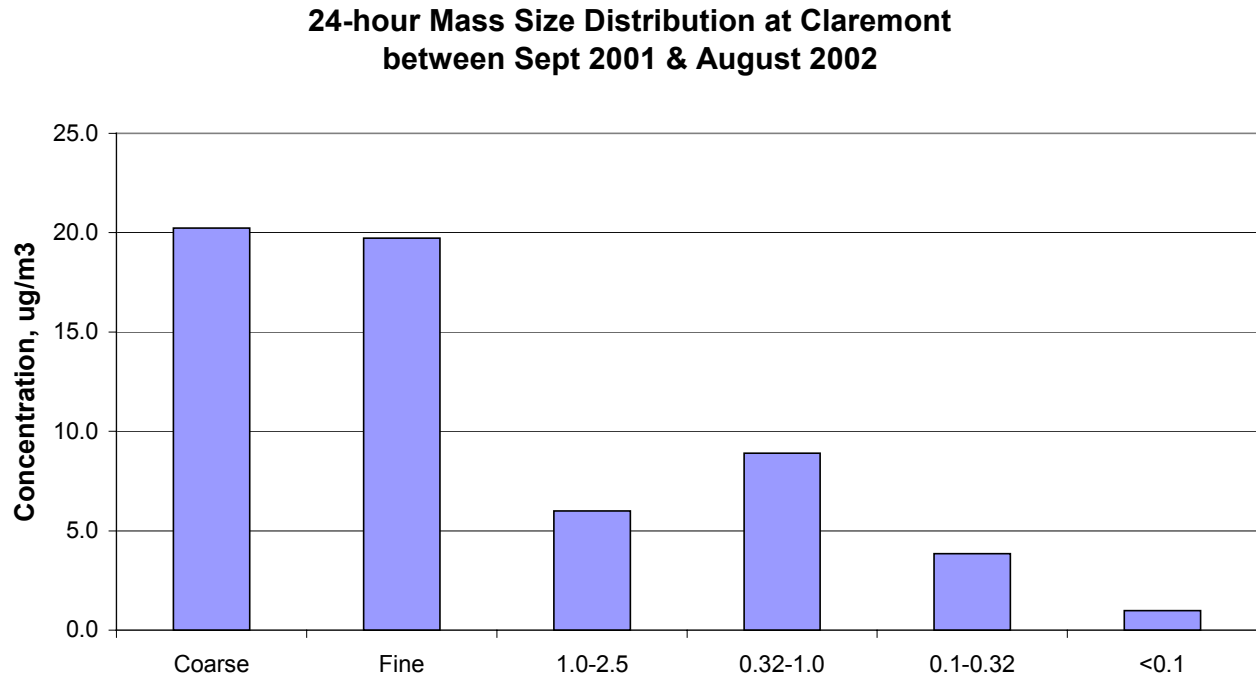


Table 1. Summary of mass and chemical concentrations by size fraction.

				<b>1.0-2.5</b>	<b>0.32-1.0</b>	<b>0.1-0.32</b>	<b>&lt;0.1</b>
		<b>Coarse</b>	<b>Fine</b>	<b>Intermed- iate</b>	<b>Droplet (Accuml')</b>	<b>Condensation (Accumulation)</b>	<b>Ultrafine</b>
<b>Average Mass</b>	<b>From 9/28/01 Period to Sampler</b>	<b>ug/m3 Partisol*</b>	<b>ug/m3 MOUDI</b>	<b>ug/m3 MOUDI</b>	<b>ug/m3 MOUDI</b>	<b>ug/m3 MOUDI</b>	<b>ug/m3 MOUDI</b>
<b>Mass</b>	(8/21/02)	20.2	19.7	6.0	8.9	3.9	0.98
Mass	(6/25/02)	19.7	19.3	5.9	8.7	3.7	1.04
<b>Mass</b>	(6/4/02)	18.7	19.1	5.7	8.7	3.6	1.02
<b>NH4NO3</b>	(8/6/02)	3.961	5.728	2.506	2.740	0.471	0.011
<b>(NH4)2SO4</b>	(8/6/02)	0.635	3.005	0.738	1.526	0.560	0.181
<b>Elemental Carbon</b>	(6/25/02)	0.053	0.594	0.023	0.111	0.230	0.232
<b>Organic Carbon</b>	(6/25/02)	1.175	4.962	0.731	1.780	1.534	1.528
<b>Metal Oxides</b>	(6/4/02)	7.0314	2.2378	0.9634	0.4971	0.2826	0.4948
<b>Elements (P, Cl, Br)</b>	(6/4/02)	0.1087	0.0286	0.0169	0.0069	0.0026	0.0018
<b>Chemical Sum**</b>		<b>12.9645</b>	<b>16.5563</b>	<b>4.9770</b>	<b>6.6616</b>	<b>3.0795</b>	<b>2.4485</b>
<b>(Chem Sum/Mass***)</b>		<b>0.6589</b>	<b>0.8577</b>	<b>0.8428</b>	<b>0.7699</b>	<b>0.8300</b>	<b>2.3636</b>

\* Partisol used for Coarse fraction, except MOUDI used where characters are highlighted in Blue

\*\* Sum from 9/28/02 through 6/25/02, except for Metals, where lab analysis is through 6/04/02.

\*\*\* For comparison purposes, Mass data through 6/25/02 is used.

### 24-Hour Chemical Size Frationation, Claremont

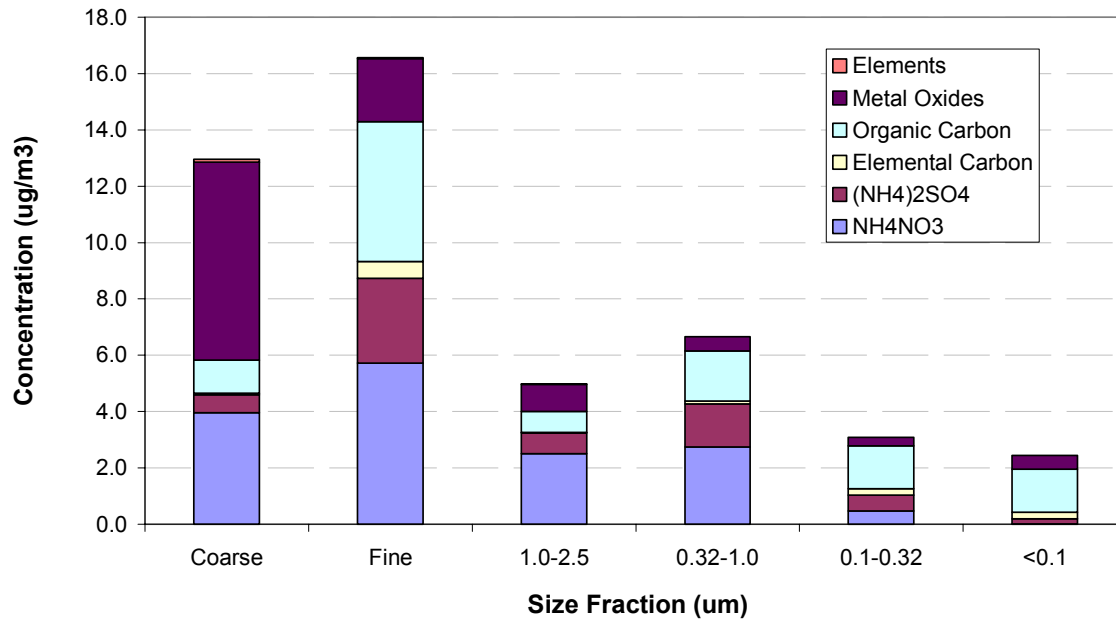


Figure 3. Chemical size speciation of 6 chemical groups.

### 24-Hour Chemical Size Frationation, Claremont

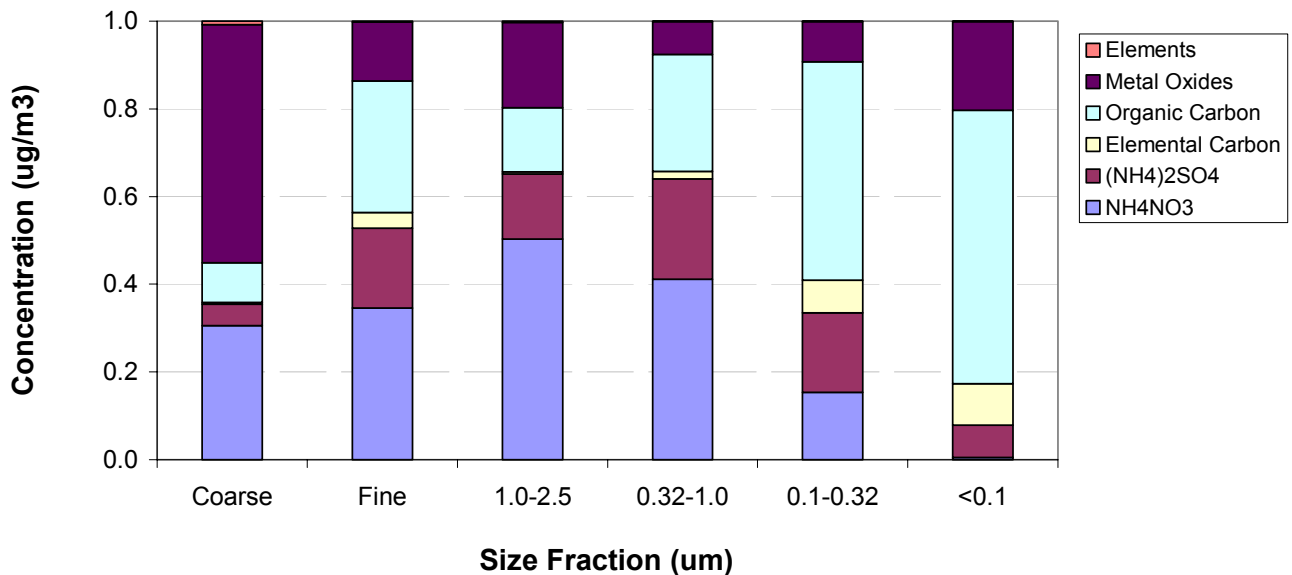


Figure 4. Relative chemical size speciation of 6 chemical groups.



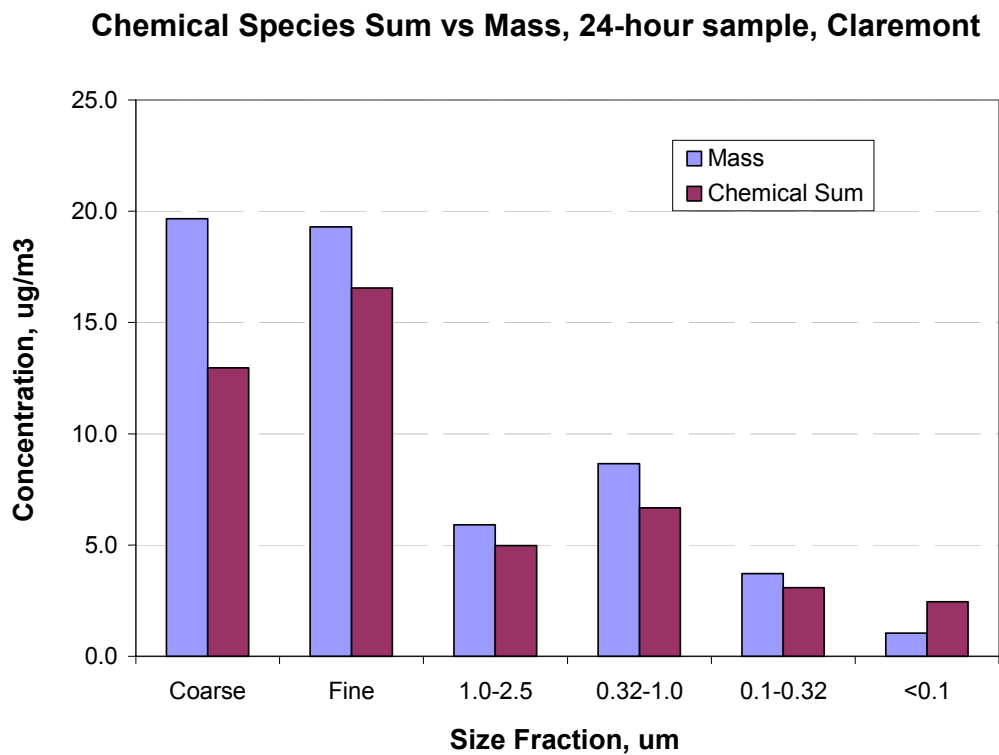


Figure 5. Comparison of Size speciated mass to the sum of all measured compounds.

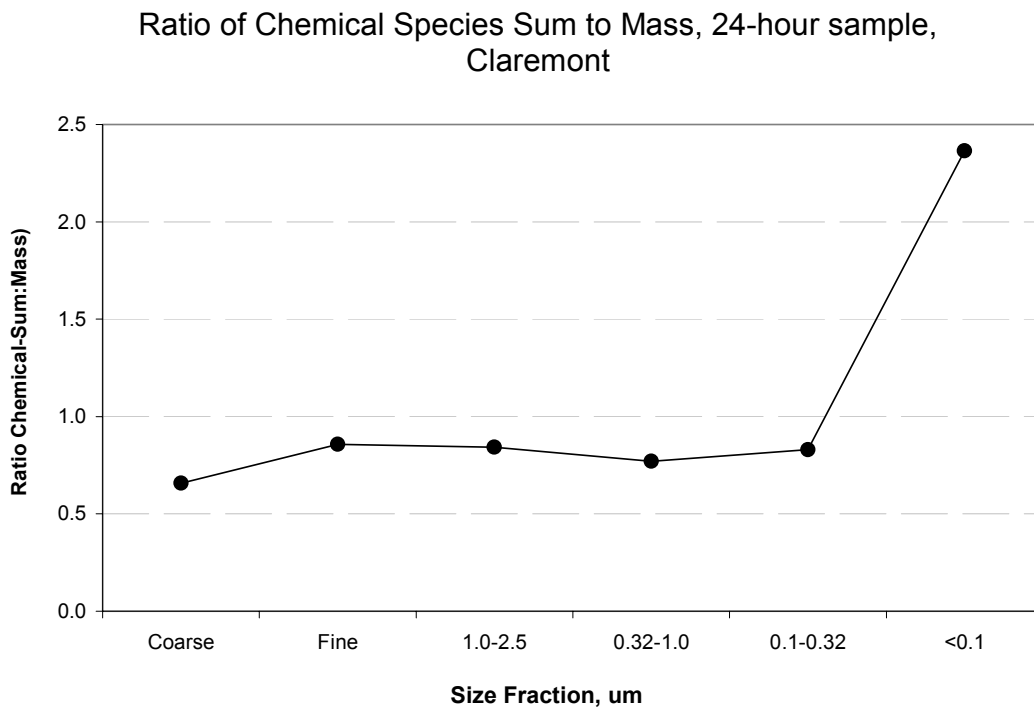


Figure 6. Ratio of the sum of all measured compounds to total mass, by size fraction.

## **5. Development and Evaluation of a PM<sub>10</sub> Impactor-Inlet for a Continuous Coarse Particle Monitor**

### **INTRODUCTION**

The development of a continuous coarse (2.5 – 10 µm) particle mass (PM) monitor can provide reliable measurements of the coarse mass (CM) concentrations in time intervals as short as 5-10 minute. The operating principle of the monitor is based on enriching CM concentrations by a factor of about 25 by means of a 2.5 µm cutpoint round nozzle virtual impactor, while maintaining fine mass, i.e., mass of PM<sub>2.5</sub> (FM) at ambient concentrations. The aerosol mixture is subsequently drawn through a standard TEOM, the response of which is dominated by the contributions of the CM, due to concentration enrichment. Findings from the field study ascertain that a TEOM coupled with a PM<sub>10</sub> inlet followed by a 2.5 µm cutpoint round nozzle virtual impactor can be used successfully for continuous CM concentration measurements.

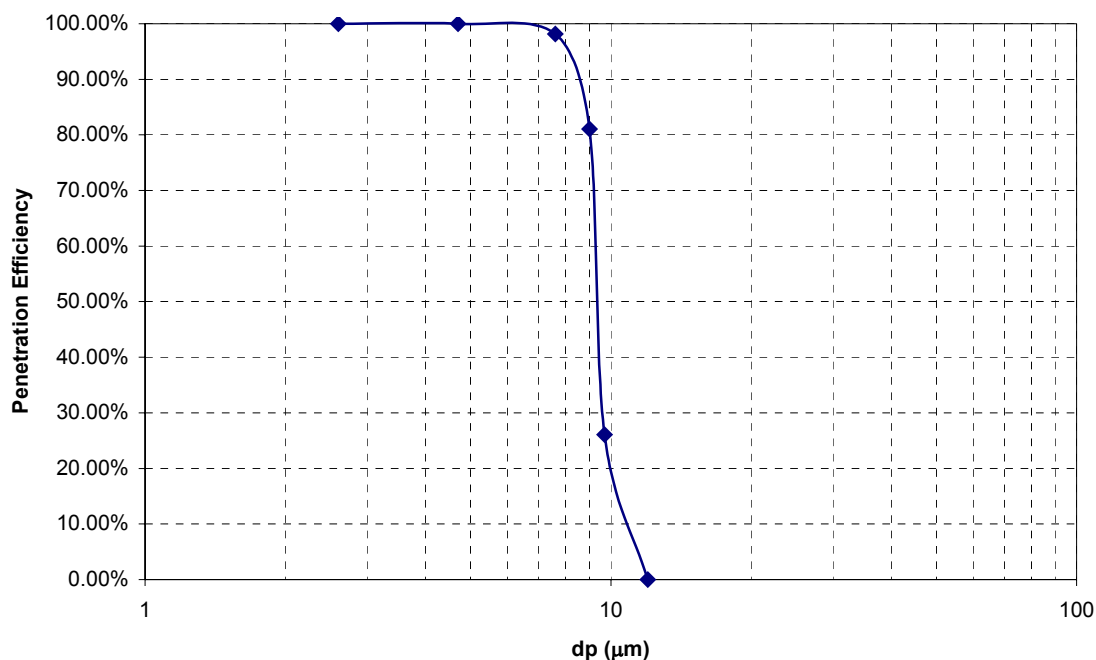
The conventional PM<sub>10</sub> inlets available operate at a flow are of 16.7 lpm (liters per minute). The purpose of this study was to develop and test a PM<sub>10</sub> designed to operate at 50 lpm which could be used for the Continuous Coarse Particle Monitor (CCPM). For this purpose the existing PM<sub>10</sub> inlet operating at 16.7 lpm was modified. The choice of the sampling flows as well as the nozzle design parameters was made so that the predicted 50% cutpoint of the impactor will be about 10 µm.

### **METHODS AND RESULTS**

#### **Lab Characterization**

The 50 lpm PM<sub>10</sub> inlet was first tested in the laboratory. Particle penetration through the impactor was measured as a function of particle size by means of a nephelometer, DataRAM (RAM-1, MIE Inc., Billerica, MA), which was used to measure the mass concentrations of the monodisperse upstream and downstream of the PM<sub>10</sub> inlet. The result of this test is shown in Figure 1. The data plotted in this figure indicate that particle penetration is 90% or higher for particles in the range of 2.5 to 8 µm. Penetration decreases sharply to about 50% at 9.5-9.7 µm and further to less than 10% for particles larger than 11 µm in aerodynamic diameter.

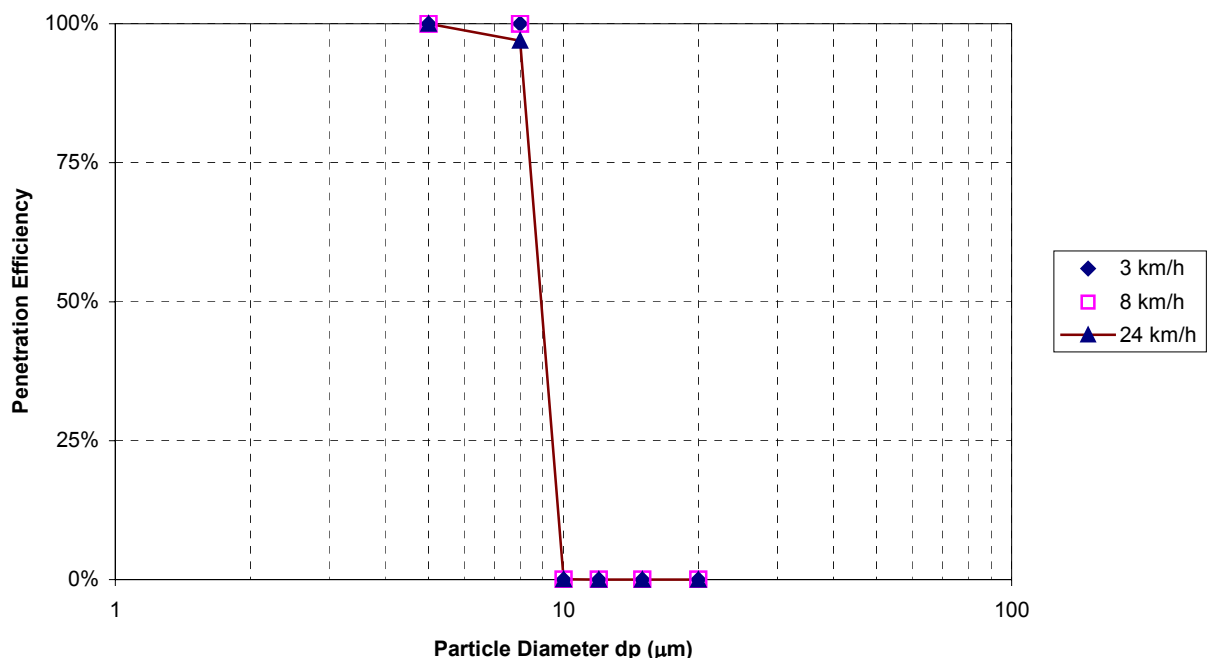
Figure 1. PM-10 Inlet Penetration Efficiency Curve



## Wind Tunnel Test

The PM<sub>10</sub> inlet was tested for collection efficiency at wind velocities of 3, 8 and 24 km/h in a Wind Tunnel facility at UCLA. Three isokinetic samplers operating at 10 lpm were used as reference samplers. Fluorescent particles were generated for various sizes and their penetration was determined as a function of wind velocity. Figure 2 shows the results of these tests. As evident from the figure, the particle penetration characteristics of the PM<sub>10</sub> inlet are unaffected by the wind speeds. The penetration for all the wind speeds tested, viz., 3, 8 and 24 km/h show a very close agreement. This is particularly important because it demonstrates that the inlet can be used throughout the various ambient conditions found in all normal environments. The wind tunnel tests show that the 50% cut is slightly shifted towards left at around 9  $\mu\text{m}$

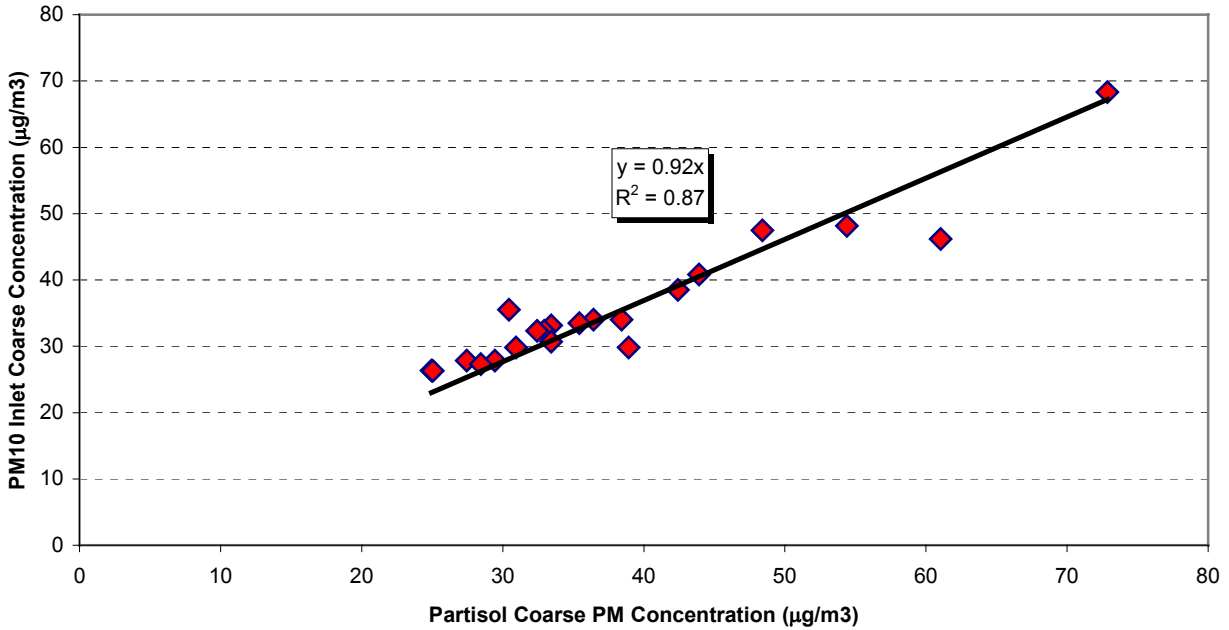
Figure 2. Plot of Penetration vs Particle Diameter for Various Wind Speed



## Field Tests

The performance of 50 lpm  $\text{PM}_{10}$  inlet was evaluated at Rubidoux, CA. For this purpose, a 2.5  $\mu\text{m}$ , round nozzle virtual impactor was connected downstream of  $\text{PM}_{10}$  inlet. Particles penetrating the  $\text{PM}_{10}$  inlet and thus having an aerodynamic diameter (AD) less than 10  $\mu\text{m}$  were drawn through the virtual impactor, which was designed to have a theoretical 50% cut point at about 2.5  $\mu\text{m}$  for an intake flow rate of 50 lpm. Coarse particles follow the minor flow, while particles smaller than the cutpoint of the virtual impactor follow the major flow. The minor flow in these experiments was set at 2 lpm to achieve a nominal enrichment factor of 25. A 47 mm Teflon filter placed after the virtual impactor collected the enriched mass. The enriched concentration obtained from the  $\text{PM}_{10}$  inlet was compared to co-located Dichotomous Partisol-Plus (Model 2025 Sequential Air Sampler, Rupprecht and Patashnick Co. Inc., Albany, NY). The Partisol uses a  $\text{PM}_{10}$  inlet operating at 16.7 lpm to remove particles larger than 10  $\mu\text{m}$  in AD. Two separate flow controllers maintain the coarse mass at 1.67 lpm and the fine mass stream at 15 lpm. Coarse and fine PM are collected on two 4.7cm Teflon filters, placed in the minor and major flows of the Partisol virtual impactor, which are housed in reusable cassettes. Figure 3 shows the comparison between coarse PM mass concentrations between the  $\text{PM}_{10}$  inlet and the Partisol. As the results show, a very good agreement persists between the two samplers. The geometric mean  $\text{PM}_{10}$  inlet to Partisol coarse PM concentration ratio is around 0.94. Coarse PM concentrations determined by both samplers appear to be also highly correlated with  $R^2=0.87$ .

**Figure 3. Coarse PM Concentrations Determined by the 50 LPM PM-10 Inlet and the R&P Partisol**



The comparison between coarse PM concentrations for crustal metals as well as ions such as nitrate and sulfate was also done between the PM<sub>10</sub> inlet and the Partisol. Figure 4 depicts an overall comparison of five crustal metals. As seen, an excellent correlation with a ratio of 0.9811 ( $R^2=0.8419$ ) persists between coarse PM metal concentration measured by Partisol and the PM<sub>10</sub> inlet. The comparison of coarse PM nitrate and sulfate concentrations measured by Partisol and the PM<sub>10</sub> inlet are shown in Figures 5 and 6, respectively. The results show a very reasonable agreement between these two samplers. Figure 5 has a slope of 0.87 while the slope for Figure 6 is 0.91. These two values are very closed to the expected ratio of 1.

Figure 4. Overall comparison between coarse PM concentration of five crustal metal measured by Partisol and PM10 inlet

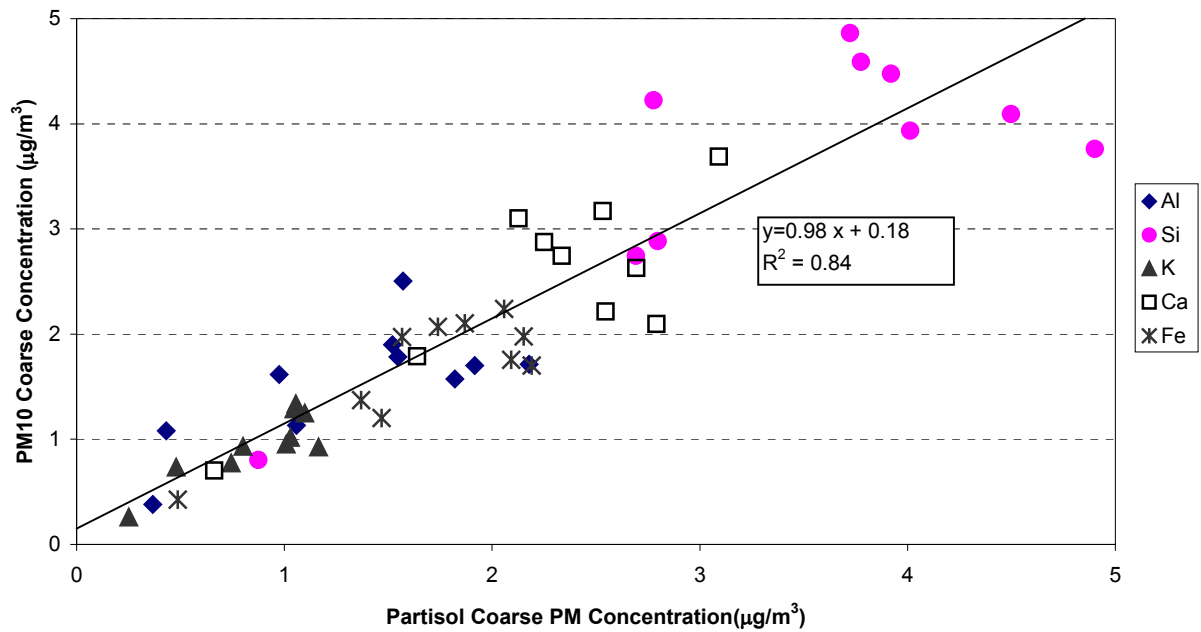


Figure 5. Plot of coarse PM nitrate concentrations between the PM10 inlet and Partisol

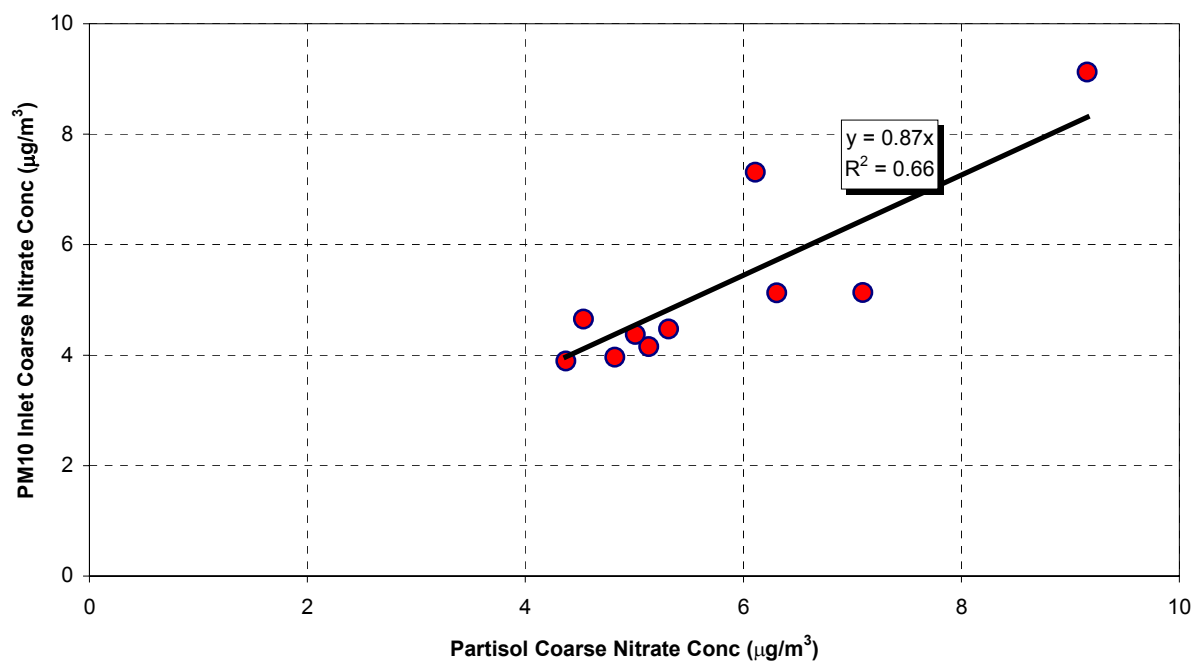
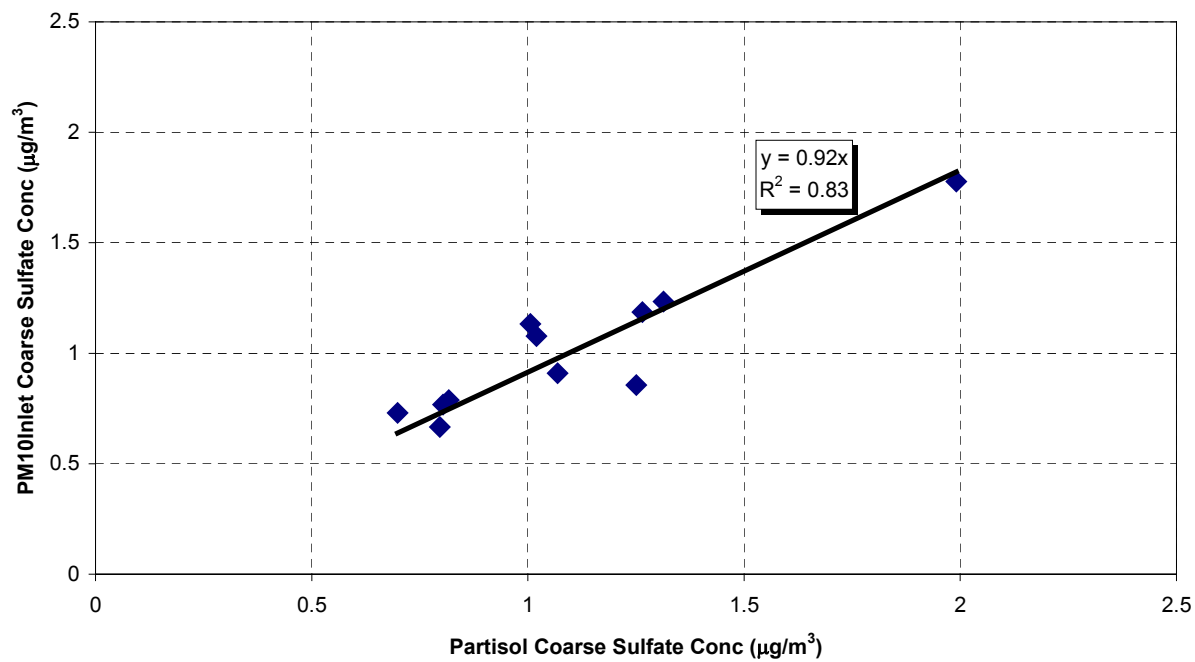
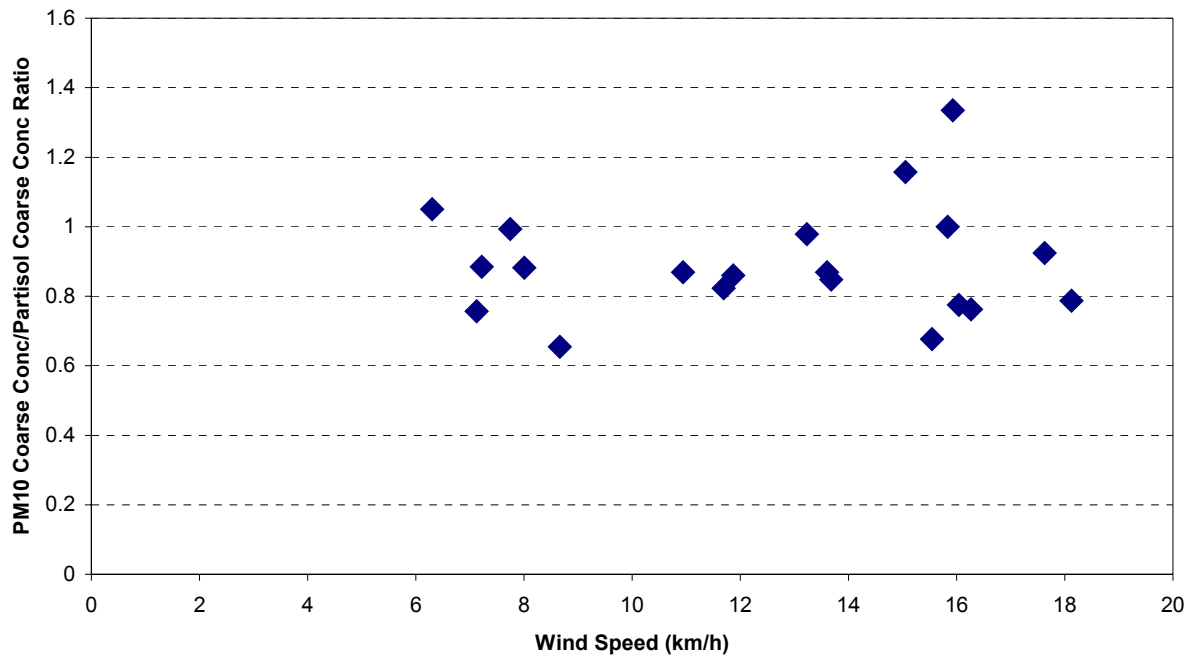


Figure 6. Plot of coarse PM sulfate concentrations between PM10 Inlet and Partisol



Finally, the coarse PM concentration ratios of PM<sub>10</sub> inlet and Partisol were plotted against the wind speed. The results shown in Figure 7 clearly indicate that the ratio is independent of the wind speed. This result further supports the findings of the wind tunnel tests and establishes the applicability of using the new 50 lpm PM<sub>10</sub> inlet in conditions of high winds.

**Figure 7. Plot of Ratio of PM10/Partisol Coarse Concentrations vs Wind Speed**





## 6. Ultrafine Organic Speciation Study

Several studies have measured individual organic compounds in atmospheric particle samples by GC/MS or other analytical methods. Usually only between 10 and 20% of the total organic compound mass (measured by thermal desorption methods) can be quantified as individual organic species. Some of these compounds can be used to trace primary particle emissions and be used in source apportionment studies. One of the major hurdles in the sampling of particles for organic speciation is collecting enough mass for the analysis. For this reason, sampling periods are very long (from 12 hours to several days) and they do not provide size-fractionated information on the organic particle concentrations. The one study that measured size-fractionated speciated organics only looked at PAH and oxy-PAH and sampled over 5 - 24 hour periods (J. Allen et al., 1996, 1997, 1998).

A new particle slit impactor developed by Dr. Sioutas and his group (Misra et al., 2002) through funding by the Southern California Supersite enables the separation of particles with a cut point of 0.18  $\mu\text{m}$  and a very high flow rate of  $\sim 500$  lpm. Using a 2.5  $\mu\text{m}$  inlet, particles with diameters between 0.18  $\mu\text{m}$  and 2.5  $\mu\text{m}$  (fine) can be collected by impaction on this new impactor, and particles with diameters less than 0.18  $\mu\text{m}$  (ultrafine) can be collected on a high-volume filter downstream. The two size fractions roughly correspond to the accumulation mode and ultrafine modes of the urban aerosol size distribution. The high flow rate of the system allows for shorter collection periods, and thus diurnal (3 1/2 - hour samples) and size-segregated sampling for organic speciation is now possible.

The sampling plan is outlined below. Briefly, two sampling sites were selected: a typical urban site (USC); and a downwind receptor site (Riverside). For one week at each site (Mon. – Fri.), four time intervals per day are sampled (morning, midday, evening, and possibly overnight). The daytime samples last 3 1/2 hours per day for each diurnal interval for five days. Nighttime sampling lasts for 1 1/2 hours per night for four nights. Filters and substrates are replaced in the sampler such that one set of accumulation mode quartz-fiber substrates and one ultrafine mode high-volume Teflon-coated glass fiber filter represent a weekly average for each diurnal interval. Parallel to the high volume sampler will be a MOUDI run at 30 lpm to collect particles on Teflon substrates for mass and potentially ion chromatography and ICP/MS analysis in the future. The stages in the MOUDI will be chosen to correspond to the same cut-points as the high volume sampler. A second MOUDI with the same flow rates and size cuts will collect aluminum foil substrates and a quartz fiber after filter for EC/OC analysis by the thermal desorption/optical transmission method used regularly by the Supersite. In addition, a 47mm filter train will consist of a PM<sub>2.5</sub> inlet, a Teflon filter and a back-up quartz fiber filter. The flow rate will be chosen to create a face velocity on the quartz back-up filter equal to the face velocity on the MOUDI quartz after filter. This filter-based sampling helps to assess the degree of organic vapor adsorption onto the MOUDI quartz after filter.

An additional high volume sampling system, operated by Janet Arey's UCR group, will consist of a filter followed by a PUF and will be used for analysis of both semi-volatile and particle-phase PAH, oxy-PAH and nitro-PAH.

A fifth system, consisting of a nano-MOUDI running at 10 lpm, will be used to collect samples at each site for ultrafine, size-segregated, PAH and quinone analysis by Tony Miguel. In order to collect sufficient mass, the nano-MOUDI runs for full 11 1/2 hour daytime and nighttime periods that correspond to the three daytime and nighttime intervals of the other samplers.

The purpose of this project is several-fold. First, with the exception of the one study on PAH and oxy-PAH, the speciated organic composition of ultrafine particles has not been investigated. Several other classes of compounds, including alkanes, substituted phenols, alkenes, alkanolic acids and diacids, aromatic carboxylic acids, resin acids, sugars and furans have been found in atmospheric particles but their distribution among size fractions is unknown. Ultrafine particles consist of fresh particles emitted directly from sources, freshly condensed material on these primary particles, and freshly nucleated particles resulting from atmospheric reactions. It has also been shown that ultrafine particles consist of up to 80% - 90% organic carbon. Source profiles for many of the organic compounds of interest have been previously determined for the most important particle sources in Los Angeles (Schauer Thesis, 1998). Furthermore, smog chamber studies have identified many particle phase organic atmospheric reaction products that should also be found in the atmosphere.

By comparing individual ultrafine organic species to known organic source profiles and expected atmospheric reaction products, the sources and formation mechanisms of these ultrafine particles can be determined. Recent data suggesting that ultrafine particles may be more toxicologically potent than larger particles provide even more motivation for this study. First identifying the origin, the geographical distribution, and the diurnal and seasonal variations of these particles will help to model personal exposure and to formulate any future pollution control efforts. Second, the toxicological effects of the ultrafine aerosol as a whole can be compared to the toxicity of the identified organic components. The sampler can also be used to collect extra ultrafine material for subsequent toxicity assays performed by Drs. Nel and Cho at UCLA.

By also looking at the organics on the accumulation-mode filter sample, the contributions of primary particle sources and secondary organic aerosol to the two particle size fractions can be resolved over the course of the day and as air parcels move across the LA basin. The organic components of the accumulation-mode particles will also have toxicological implications, and can be compared to the organic components found in the ultrafine fraction.

Finally, the warm weather and large number of pollution sources in the LA basin create ideal conditions for secondary organic aerosol (SOA) formation. A goal of this study is to identify as many individual components of the SOA as possible. This will provide much needed data to smog chamber experimenters and SOA formation modelers. The temporal and spatial aspects of this study will shed additional light on SOA formation mechanisms.

### Experimental Matrix

Two sites: Urban (USC), and Receptor (UC Riverside)

One week (five days) at each sampling site for each season

Four time intervals each day: 7AM - 10:30AM, 11:00AM – 2:30PM, 3PM –6:30PM, and 7:00PM – 6:30AM

Weather conditions and traffic patterns should remain constant throughout each week, and preferably, throughout the entire study.

When: August, to maximize effect of photochemistry; and December, a low photochemical and cold weather sample

### Progress

The first round of sampling has recently been completed. From August 12 to August 16, 2002, sampling was conducted on the rooftop of a 3-story building at the University of Southern California campus (urban site). From August 26 to August 30, 2002, sampling took place at the University of California, Riverside Citrus Research Center and Agricultural Experiment Station (CRC-AES) adjacent to an existing SCAQMD air sampling facility (receptor site). Filters are currently in the process of being weighed and analyzed. Planning has begun for the wintertime tests, again at USC and Riverside. Sampling is tentatively scheduled for the end of November and the beginning of December.

## **7. Particle Size Distribution of Polycyclic Aromatic Hydrocarbons, Elemental Carbon, and Organic Carbon Measured in Claremont: Part I Seasonal Variations from October 2001 to May, 2002**

### **Summary**

This report (Part I) describes an eight-month set of measurements of the size distribution of twelve priority pollutant polycyclic aromatic hydrocarbons (PAH), EC and OC measured from October 2001 to May, 2002 in Claremont, a receptor site located about 40 km downwind of central Los Angeles. The next report (Part II) will describe the results obtained during June, July and August, thus completing a full year of measurements. Samples were collected once every week, for 24-hr periods, from midnight to midnight. A MOUDI impactor with four or five stages collected samples at 30 LPM which were composited into monthly periods into three aerodynamic diameter size intervals: 0-0.18  $\mu\text{m}$  (ultrafine mode I), 0.18-2.5  $\mu\text{m}$  (accumulation mode II), and 2.5-10  $\mu\text{m}$  (coarse mode III). PAH were separated and quantified by gradient HPLC with selective fluorescence detection; EC and OC were measured using a thermo-evolution/optical transmission carbon analyzer. The effects of season temperature on the size distributions and total mass of the measured species are briefly discussed. The full effects of season, including RH, and the reactivities of individual PAH will be evaluated in Report II. This may be the first set of data that includes measurement of both PAH and OC on the same sample.

### **Background**

Recent studies have reported that, during transport across the Los Angeles basin, after emission from combustion sources, the size distribution of PAH undergo changes from smaller to larger modes (Eiguren-Fernandez et al., 2002, Venkataraman and Friedlander, 1994). The processes responsible for these changes are not well understood but have been hypothesized to result from several factors, including the concentration of several species present in the air parcel, aerosol dynamics, phase partitioning, photochemical reactions, and meteorology.

PAHs emitted by vehicular emissions are associated with fine elemental carbon (EC). It has been shown that EC concentrations in urban ambient air are dominated by emissions from diesel engines including both on-highway and off-highway applications (Gray and Cass, 1998). Thus, EC constitutes a chemically and physically stable tracer of diesel emissions. On the other hand, Gray and Cass (1998) reported that EC+OC (total particulate carbon) result from the accumulation of small increments from a great variety of emission source types including both gasoline and diesel powered highway vehicles, stationary source fuel oil and gas combustion, industrial processes, paved road dust, fireplaces, cigarettes and food cooking (e.g. charbroilers).

EC and OC account for the major fraction of mass of carbonaceous particles present in ambient air. For this reason, detailed measurements of the distribution of EC, OC and PAH as a function of particle size and season may help improve our understanding of the processes that govern observed changes in their size distributions during regional transport. Changes in particle size distributions modify their dry and wet deposition, atmospheric residence time, and deposition efficiency in the human respiratory system.

The results presented in this preliminary assessment of the data available to date are evaluated with a focus on the effects of ambient temperature seeking an understanding of the processes that are responsible for the observed changes in the size distributions of PAH, EC and OC measured at a receptor site.

## EXPERIMENTAL SECTION

**Sample Collection and Sites.** Sampling was carried out for 24-hr periods every week from midnight to midnight, during an eight-month period in Claremont starting October, 2001. At this downwind site, primary and secondary PM are mixed with wind blown dust from the nearby deserts. In addition, PM originally emitted in urban Los Angeles is advected into the Claremont area after several hours of atmospheric transport. We therefore refer to the Claremont air pollution regime as a “receptor” area of the Los Angeles Basin. Samples were collected using a four- or five-stage Microorifice Uniform Deposit Impactors (MOUDI Model 110, MSP Corp., Minneapolis, MN). For analysis, monthly samples were composited into three aerodynamic diameter size intervals: 0-0.18  $\mu\text{m}$  (ultrafine mode I), 0.18-2.5  $\mu\text{m}$  (accumulation mode II), and 2.5-10  $\mu\text{m}$  (coarse mode III). Particles were deposited on un-coated pre-baked aluminum foils (accumulation mode) and quartz filters (coarse and ultrafine mode) using a MOUDI impactor. These size bins were chosen to allow quantification of the target PAHs in 24 hr samples, while collecting particles in the ultrafine, accumulation and coarse modes. An uncoated 47 mm dia. quartz fiber filter (Pallflex Corp., Putnam, CT) was used as an impaction substrate for the 10  $\mu\text{m}$  cut point stage of the MOUDI to remove particles larger than 10  $\mu\text{m}$ .

**PAH Extraction.** The impaction substrates corresponding to each size interval monthly composite were placed in amber vials with a Teflon-lined caps and extracted with 15 mL of dichloromethane (DCM) by ultrasonication for 24 min and then filtered using 5.0  $\mu\text{m}$  nylon membrane filters. The filter extracts were solvent exchanged by adding 0.1 mL of acetonitrile to a 1 mL aliquot of the DCM extract followed by volume reduction (without drying!) to ~0.1 mL by evaporation at room temperature inside an empty desiccator. The exact reduced volume was measured with a chromatographic syringe.

**PAH Separation and Quantification.** PAHs were separated by HPLC and measured by a scannable fluorescence detector. The PAH excitation and fluorescence emission conditions used were optimized to obtain the highest sensitivity. Details of the procedure were previously reported, and are described elsewhere (Eiguren-Fernandez and Miguel, 2002). NIST SRM 1649a standard was used as positive control. PAH amounts found in the blanks (aluminum foils and quartz filters) were subtracted from the sample values, thus defining the limit of detection of the analytical protocol. The instrument detection limit (IDL) at an S/N ratio = 5 for a 20  $\mu\text{L}$  injection of the PAH ranged from 0.3 to 18 pg. Method standard deviations for the 15 target PAHs running triplicate analysis of the as positive control standard (SRM 1649a) averaged 8.0% and ranged from 3.8 to 15%. Correlation coefficients  $r^2 \geq 0.999$  were obtained with five-point calibration injections in the range of the expected PAH concentrations.

## RESULTS AND DISCUSSION

The target PAH studied were grouped according to their sub-cooled vapor pressure,  $p_L^o$ . The group of semivolatile PAH ( $\log[p_L^o]$  from -0.95 to -2.06) includes PHE, ANT, PYR, and FLT. The group of less volatile PAH ( $\log[p_L^o]$  from -3.22 to -7.04) includes BAA, CRY, BGP, BAP, BBF, BKF, DBA and IND. Their names, MW, and individual sub-cooled liquid vapor pressures are listed in Table 1, along with the detection limits of the HPLC method.

**Normalized EC and OC Size Distributions.** Normalized EC and OC size distributions and total mass (M) measured in Claremont from November 2001 to May, 2002, are presented in Figures 1 and 2. The EC distributions are distinguished by prominent modes in the ultrafine and accumulation size interval during the entire period. Coarse modes were not observed for EC during this period. OC distributions also showed significant accumulation modes in all samples, and a smaller ultrafine mode for most samples. Definite differences were also observed: For instance, one sample (May 2002) showed a small OC coarse mode, while another sample (March 2002) showed a small OC ultrafine mode. Hypotheses that may explain these distributions are given in a separate section below.

**Normalized PAH Size Distributions.** Normalized PAH group size distributions and total mass (M) measured in Claremont from November 2001 to May, 2002, are presented in Figures 3 and 4. For each monthly composite, the distributions of the group that includes the semivolatile PAH (PHE-FLT) are similar to the group containing the less volatile PAH (BAA-IND). However, the distribution shapes vary quite markedly over the observed period. From October, 2001, to January, 2002, the distributions contained no coarse modes. From then on, most of the distributions showed a prominent coarse mode, for both PAH groups.

**Total PAH Concentration by Group in Modes I, II and III:** The total mass concentrations (M) of PAH in the PHE-FLT and BAA-IND group in the ultrafine, accumulation, and coarse modes, measured in Claremont from October, 2001 to May, 2002, are shown in Figures 5a and 5b, respectively. For both PAH groups, the Oct-Jan concentrations did not vary much in all 3 modes, with the largest mass (except for November) in mode II. Beginning in March, after a spike observed in February, the concentrations significantly increased in the semivolatile group, and decreased in the less volatile group (Figures 5a and 5b). In addition, during this later period, for both groups, the largest fraction of the mass moved towards the coarse mode, as compared with the previous periods.

**Total EC and OC Concentration in Modes I, II and III:** The total mass concentrations (M) of EC and OC in the ultrafine, accumulation, and coarse modes, measured in Claremont from October, 2001 to May, 2002, are shown in Figures 6a and 6b, respectively. The EC concentrations decrease from October to January, and increase from then on (Figure 6a). The ultrafine and the accumulation modes contain most of the EC mass (Figure 6a). In contrast, the largest fraction of the OC mass was measured in the accumulation and coarse modes (Figure 6b). During the entire period, a much larger fraction of OC mass was measured in the accumulation mode. During the entire period, the fraction of mass in the coarse mode was much higher for OC, as compared with EC.

PAH, EC and OC Total Mass Variation with Temperature: EC-OC, and PAH concentrations measured in the monthly composites are shown, along with mean temperatures, in Figures 7 and 8, respectively. The strong effect of ambient temperature on the concentrations of the measured EC and OC is clearly shown (Figure 7). The Pearson correlation coefficients ( $r$ ) of ambient temperature with total EC and OC mass are 0.67 and 0.75, respectively (Table 2). Separated by modes, the correlations ( $r$ ) are 0.84 for EC in the ultrafine mode, and 0.96 for OC in the coarse mode (Table 2). PAH concentration in the semivolatile group closely tracks ambient temperature, but not so well for the less volatile group (Figure 8).

Correlations of Mean Ambient Temperatures with PAH, EC and OC Concentrations: Figure 2 shows the Pearson correlation coefficients ( $r$ ) calculated for each mode and the total mass of PAH, EC and OC, along with MW and subcooled vapor pressures of the individual PAH. For total species mass, the highest correlations were found for OC (0.75), EC (0.67), PHE (0.60) and ANT (0.62) (Table 2). For the individual modes, the highest correlations were found in mode III for OC (0.96), mode I for EC (0.84), mode II for ANT, modes I (0.60) and II (0.59) for PHE, and modes I and II for ANT (Table 2). In all 3 modes, the correlations of temperature with EC and OC are positive.

While positive correlations were found for all PAH, EC and OC in mode III, for all PAH, except for BAA, the correlations for modes I and II were all negative. Thus, increasing ambient temperature increases the concentrations of all species in the coarse mode, and the semivolatile PAH in the ultrafine mode, PHE and ANT in the accumulation mode. With the noted exception of BAA in mode I, the concentration of all PAH associated with the ultrafine and the accumulation modes in the less volatile PAH group increase with decreasing ambient temperature. It is note worthy that both (semivolatiles) PHE and ANT have similar vapor pressures, and are ca. one order of magnitude higher than the other PAH in this group (PYR and FLT) as shown in Figure 2. Thus, their vapor-phase concentrations are much higher than that for PYR and FLT. PAH in the less volatile group have vapor pressures that are between one and five orders of magnitude lower, and thus are found mostly in the particle-phase (see Figure 9). Conversely, PAH in the semivolatile group are found predominantly in the vapor-phase (Figure 9). Given that PHE and ANT concentrations in the vapor-phase are large compared with other PAH, it is reasonable to expect that the partitioning process towards the particle-phase will occur during regional transport, and thus over a longer period of time.

### **Preliminary Conclusions on the Observed Evolution of the Size Distributions.**

When the complete data set is available for PAH, EC and OC, including concentrations during the warmer month of June, July, and August, and RH, sulfate, wind direction, potassium, and iron for the entire period, we will be better positioned to evaluate the parameters that contribute

to the observed changes in the size distributions of the measured species. Nevertheless, a few basic hypothesis are possible using the data available to date.

- EC: High positive correlation of temperature with EC in mode I suggests increased transport of diesel emissions from the central LA Basin to Claremont during the warmer months.
- OC: High positive correlation of temperature with OC in mode III suggests increased production of secondary organic particles which coagulate with coarse mode particles (sulfates grown to the coarse mode by water condensation?)
- PHE-ANT: High positive correlation suggests increased contribution from diesels, and partitioning from the vapor-phase during transport.
- BAA-IND: Negative correlations of temperature with the less volatile PAH in modes I and II suggest desorption from the particle-phase (when the temperature increases) and partitioning from the vapor to the particle-phase (when the temperature decreases). Positive correlations with mode III suggest coagulation of these PAH with coarse particles (sulfates grown to the coarse mode by water condensation?)



## Literature Cited

Eiguren-Fernandez, A. and Miguel, A. H. (2002). Determination of Semi-volatile and Particulate Polycyclic Aromatic Hydrocarbons in SRM 1649a and PM2.5 Samples by HPLC-Fluorescence. Accepted for publication in *Polycyclic Aromatic Compounds*.

Eiguren-Fernandez, A., Miguel, A. H., Jaques, P., and Sioutas, C. (2002) Evaluation of a Denuder-MOUDI-PUF Sampling System to Measure the Size Distribution of Semivolatile Polycyclic Aromatic Hydrocarbons in the Atmosphere. Accepted for publication in *Aerosol Sci. Technol.*

Gray, H. A, and Cass, G. R. (1998) Source contributions to atmospheric fine carbon particle concentrations. *Atmospheric Environment*, 32:3805-3825.

Venkataraman, C. and Friedlander, S.K. (1994) Size Distributions of Polycyclic Aromatic Hydrocarbons and Elemental Carbon. 2: Ambient Measurements and Effects of Atmospheric Processes. *Environ. Sci. & Technol.*, 28:563-572.

**Table 1. PAH codes, molecular weight, and HPLC-FL instrument detection limits.**

<b>PAH</b>	<b>Code</b>	<b>MW</b>	<b>IDL <sup>a</sup> (pg)</b>
phenanthrene	PHE	178	0.72
anthracene	ANT	178	0.31
pyrene	PYR	202	0.47
fluoranthene	FLT	202	1.29
benz[ <i>a</i> ]anthracene	BAA	228	1.04
chrysene	CRY	228	0.37
benzo[ <i>ghi</i> ]perylene	BGP	276	2.25
benzo[ <i>a</i> ]pyrene	BAP	252	0.75
benzo[ <i>b</i> ]fluoranthene	BBF	252	1.09
benzo[ <i>k</i> ]fluoranthene	BKF	252	0.32
dibenz[ <i>a,h</i> ]anthracene	DBA	278	1.32
indeno[1,2,3- <i>cd</i> ]pyrene	IND	276	18.5
<sup>a</sup> Instrument Detection Limit			

**Table 2.** Pearson coefficient (r) for the correlation of ambient temperature with PAH, EC and OC concentration in each size mode, total species mass (M), and subcooled liquid vapor pressure for the target PAH. Positive correlations are black, negative are **red**. Coefficients  $\geq 0.5$  are in bold text.

PAH properties are shown in the last two columns.

Species	Mode I	Mode II	Mode III	M	MW	(log $p^{\circ}_L$ ) <sup>a</sup>
PHE	0.60	0.49	0.59	0.60	178	-0.95
ANT	0.57	0.74	0.47	0.62	178	-1.11
PYR	<b>0.06</b>	<b>-0.09</b>	<b>0.37</b>	<b>0.22</b>	202	-1.92
FLT	<b>0.12</b>	<b>-0.41</b>	<b>0.47</b>	<b>0.21</b>	202	-2.06
group mean	<b>0.34</b>	<b>0.18</b>	<b>0.47</b>	<b>0.41</b>		
BAA	<b>0.49</b>	<b>-0.71</b>	<b>0.41</b>	<b>0.46</b>	228	-3.22
CRY	<b>-0.06</b>	<b>-0.56</b>	<b>0.37</b>	<b>-0.03</b>	228	-3.97
BGP	<b>-0.16</b>	<b>-0.33</b>	<b>0.23</b>	<b>-0.36</b>	276	-4.65
BAP	<b>-0.18</b>	<b>-0.65</b>	<b>0.27</b>	<b>-0.60</b>	252	-4.67
BBF	<b>-0.08</b>	<b>-0.40</b>	<b>0.19</b>	<b>-0.23</b>	252	-4.99
BKF	<b>-0.20</b>	<b>-0.66</b>	<b>0.24</b>	<b>-0.54</b>	252	-5.39
DBA	<b>-0.05</b>	<b>-0.62</b>	<b>0.36</b>	<b>-0.25</b>	278	-7.04
IND	<b>-0.16</b>	<b>-0.49</b>	<b>0.21</b>	<b>-0.38</b>	276	b
group mean	<b>-0.05</b>	<b>-0.55</b>	<b>0.29</b>	<b>-0.24</b>		
EC	0.84	0.58	<b>0.20</b>	0.67		
OC	0.56	0.50	0.96	0.75		

a subcooled liquid vapor pressure at 293 °K

b unknown

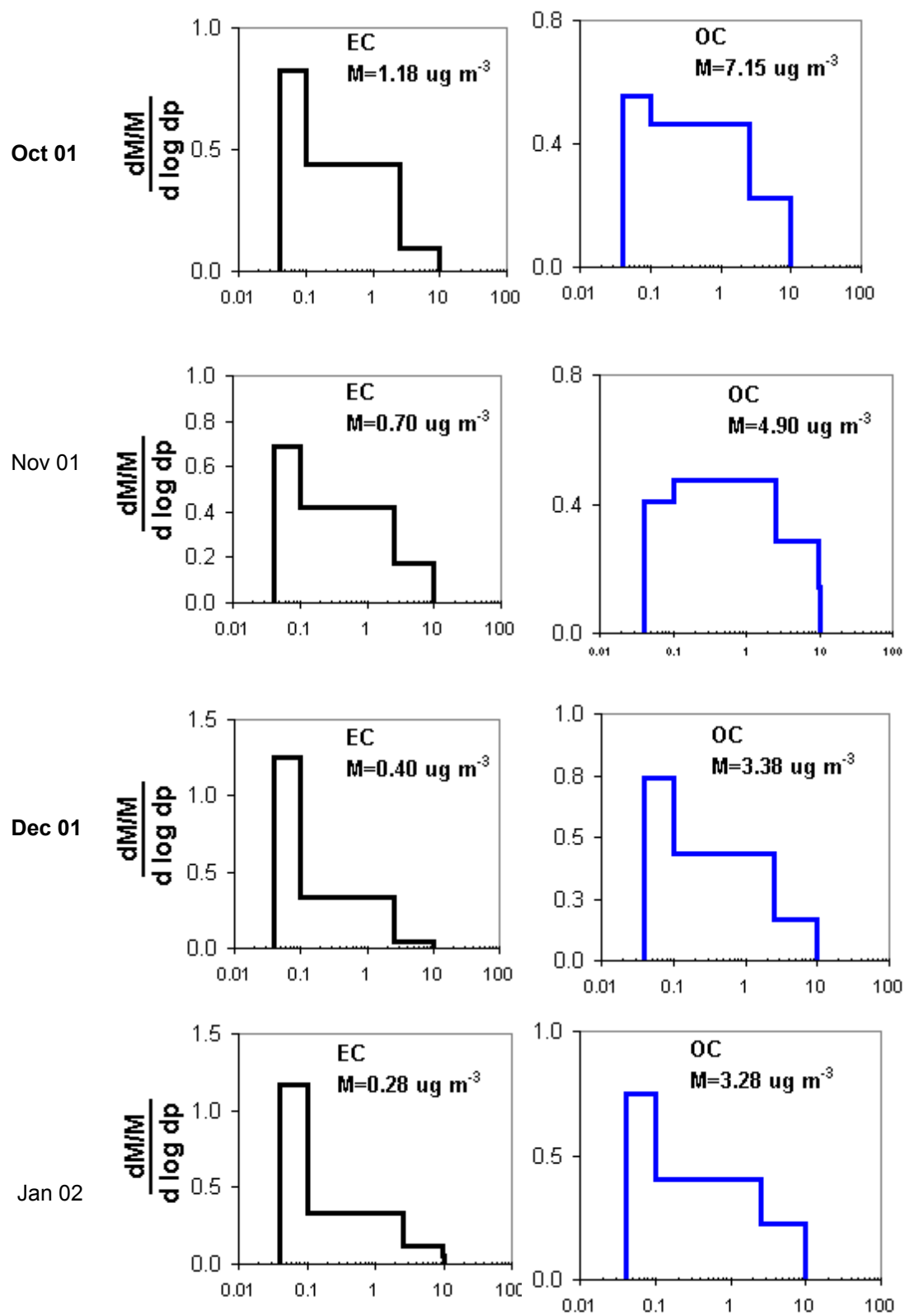


Figure 1. Size distributions and total mass concentrations (M) of EC and OC measured from October, 2001 to January, 2002 in Claremont, CA. Data obtained from monthly composites.

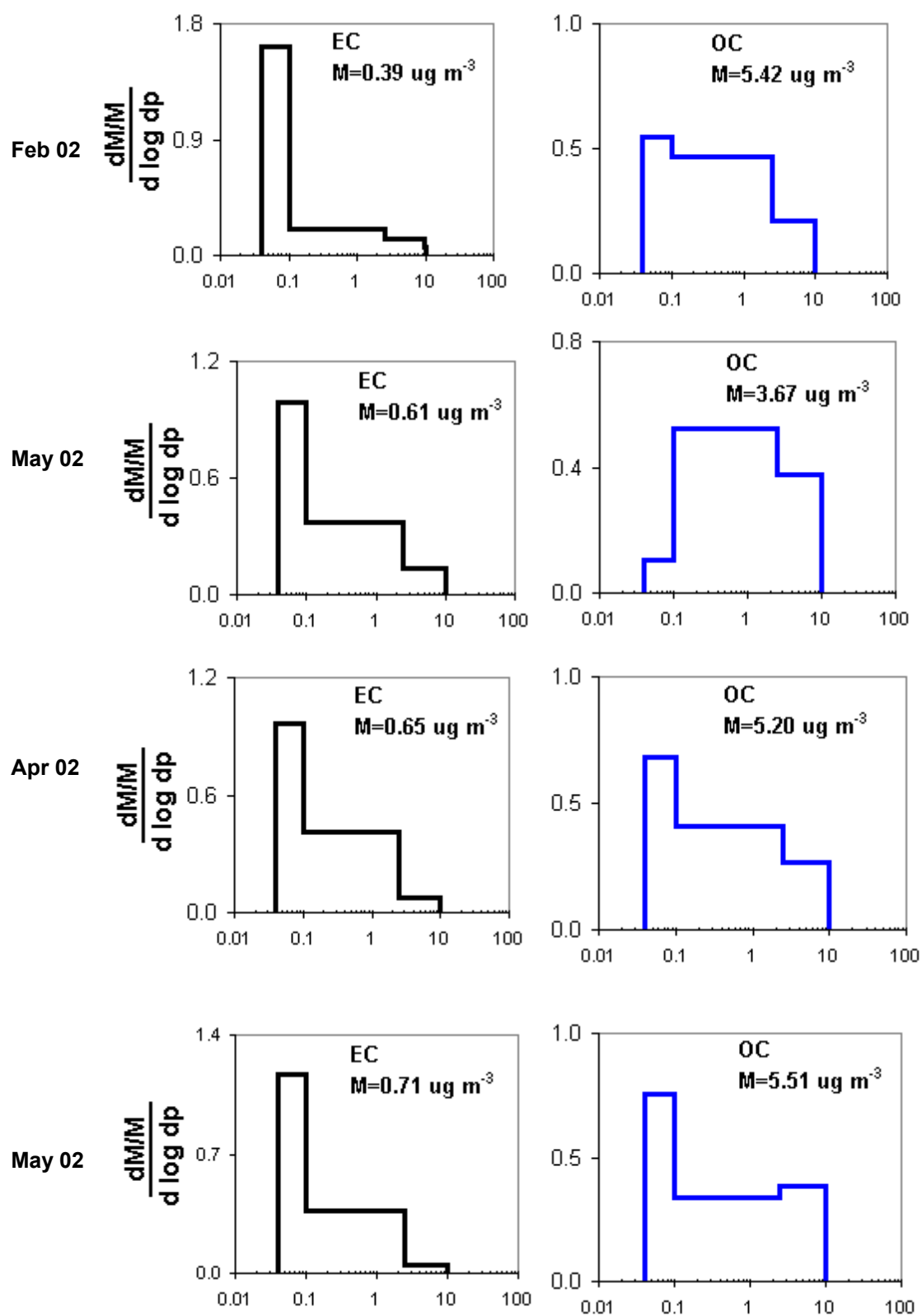


Figure 2. Size distributions and total mass concentrations (M) of EC and OC measured from February, 2002 to May, 2002 in Claremont, CA. Data obtained from monthly composites.

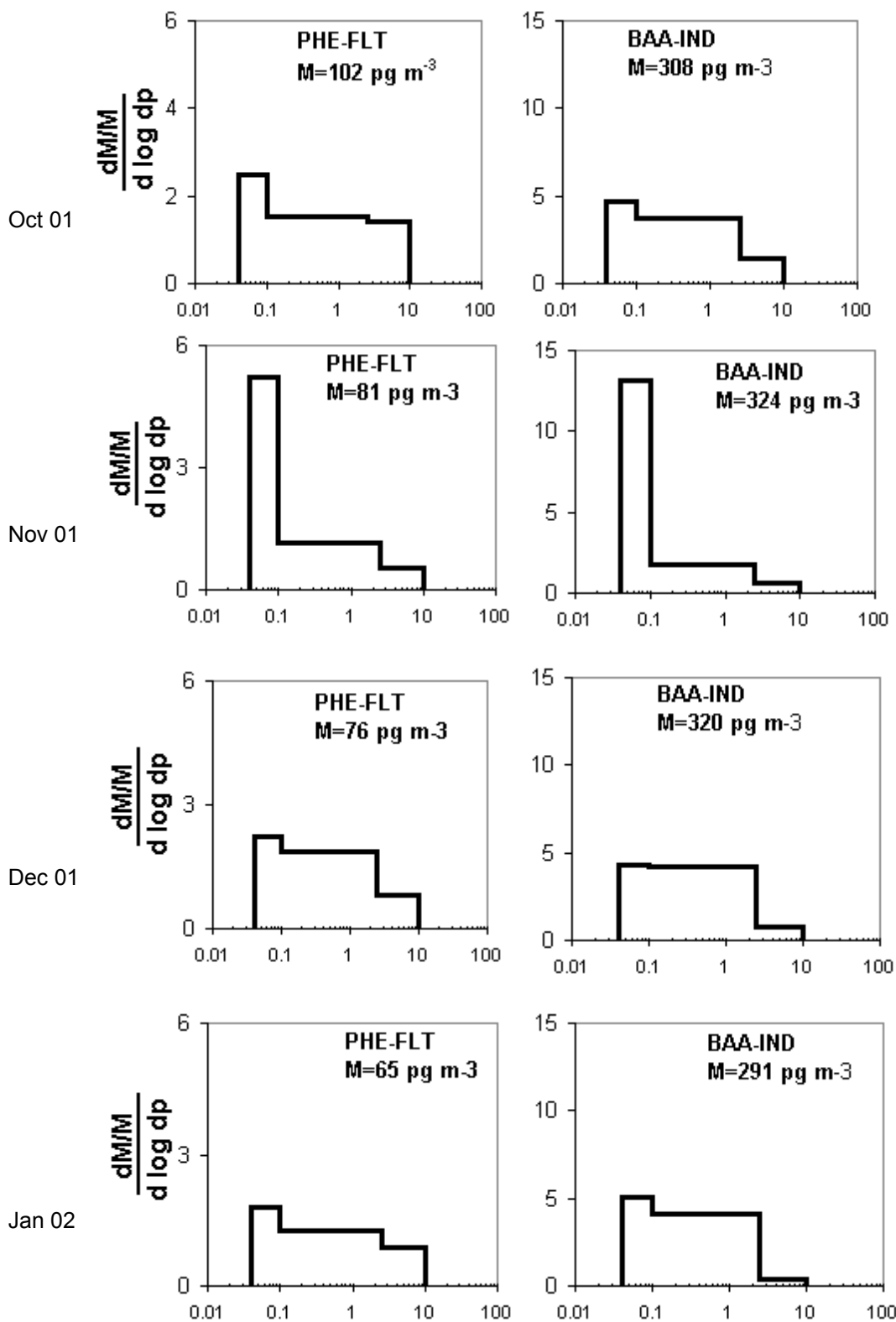


Figure 3. Size distributions and total mass concentrations (M) of PAH groups PHE-FLT and BAA-IND measured from October, 2001 to January, 2002 in Claremont, CA. Data obtained from monthly composites.

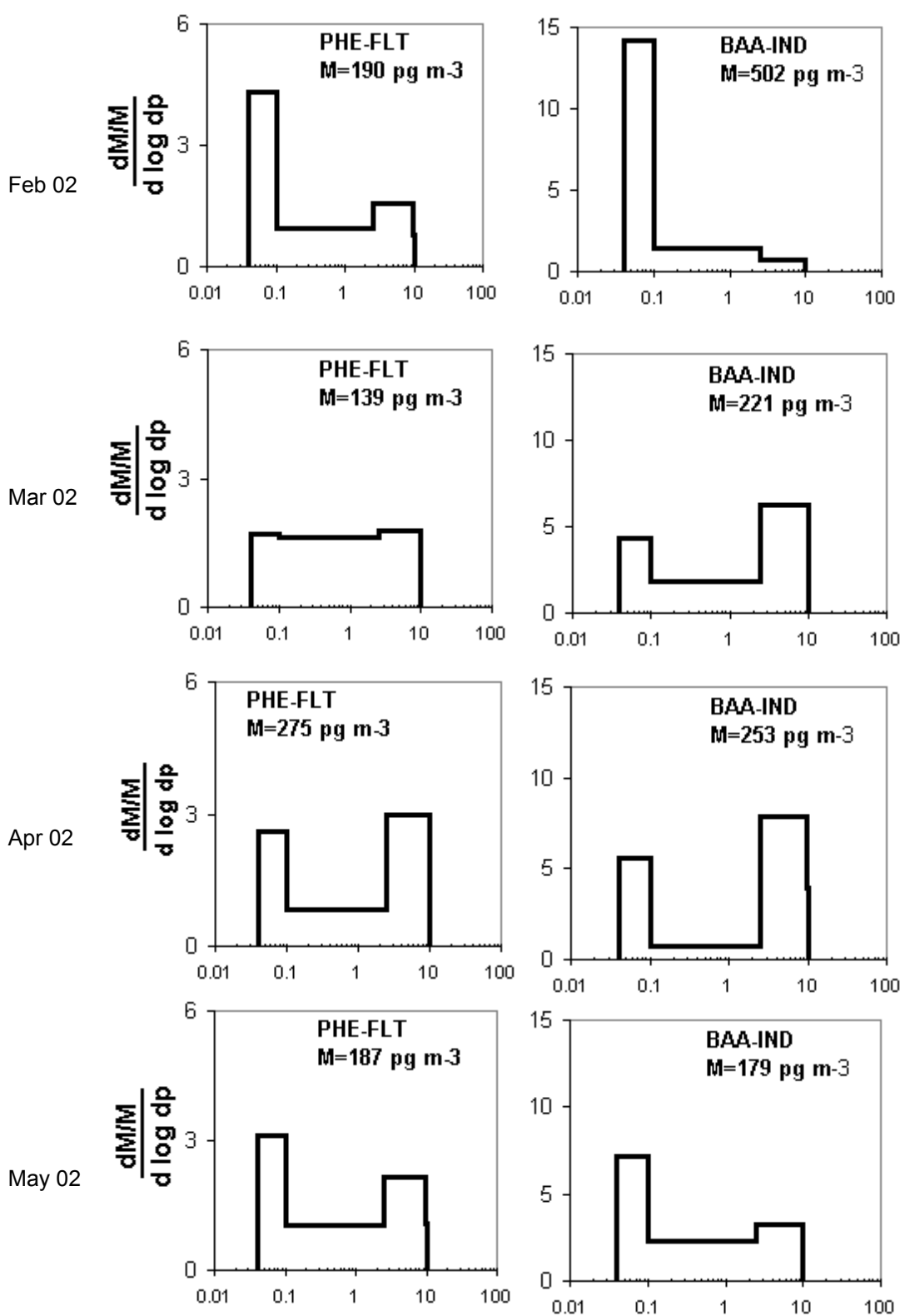
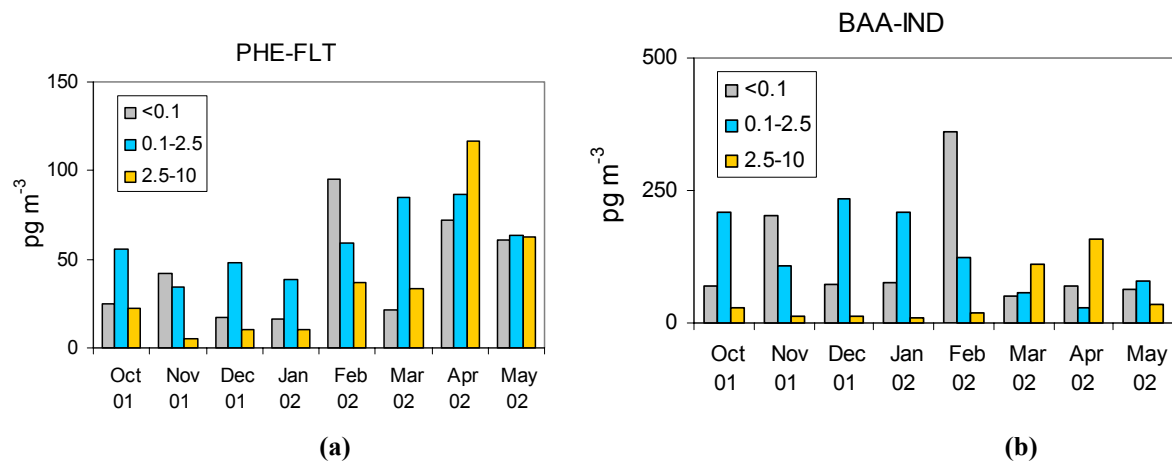
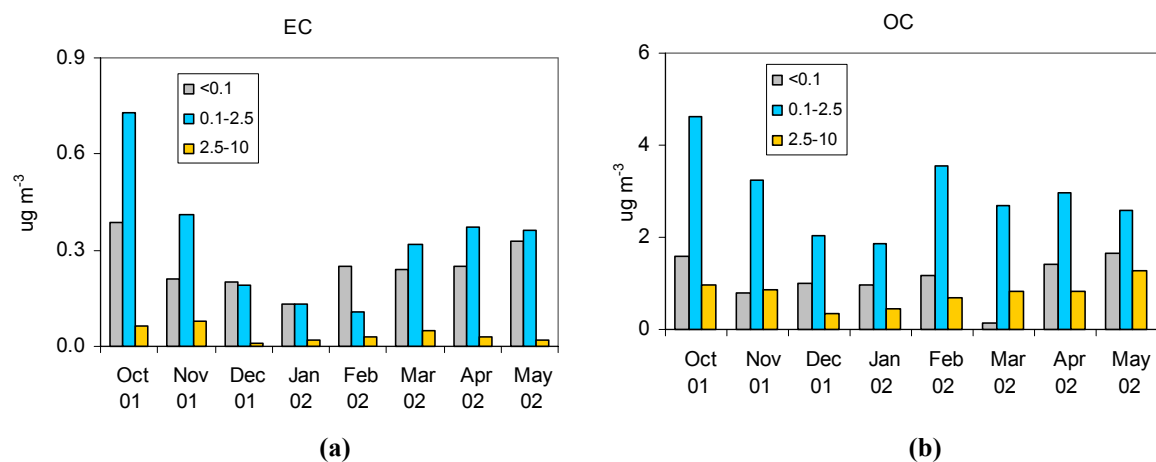


Figure 4. Size distributions and total mass concentrations (M) of PAH groups PHE-FLT and BAA-IND measured from February, 2002 to May, 2002 in Claremont, CA. Data obtained from monthly composites.



**Figure 5.** Total mass concentrations (M) of PAH in group PHE-FLT (a) and BAA-ID (b), measured in the ultrafine, accumulation, and coarse modes, from October, 2001 to May, 2002 in Claremont, CA. Data obtained from monthly composites.



**Figure 6.** Total mass concentrations (M) of EC (a) and OC (b) measured in the ultrafine, accumulation, and coarse modes, from October, 2001 to May, in Claremont, CA. Data obtained from monthly composites.



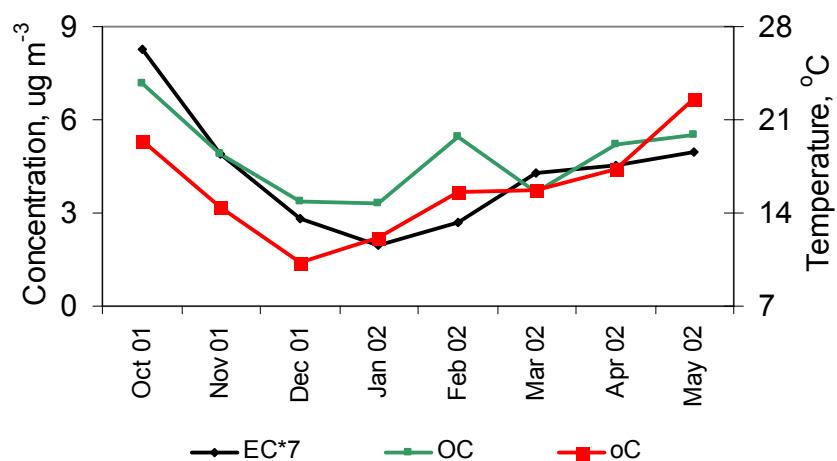


**Figure 7. Average monthly temperatures, and seasonal trends of total mass concentrations (M) of EC and OC measured from October, 2001 to May, 2002.**

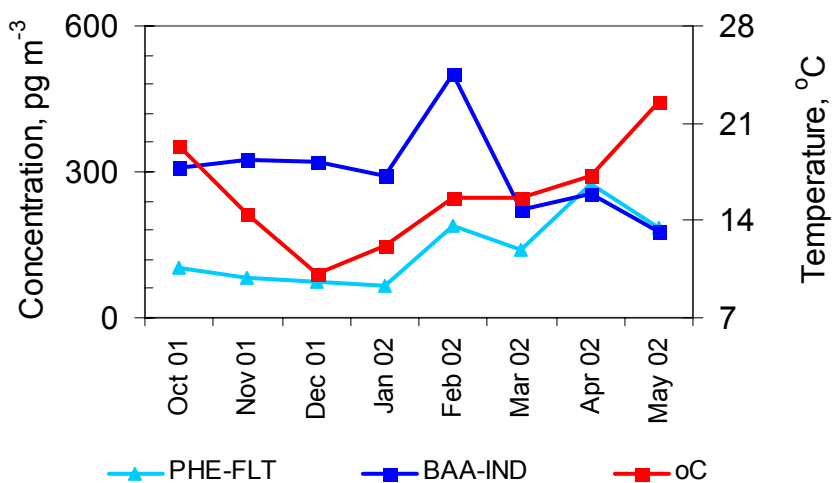


**Figure 8. Average monthly temperatures, and seasonal trends of total mass concentrations (M) of PAH groups PHE-FLT and BAA-IND, measured from October, 2001 to May, 2002.**

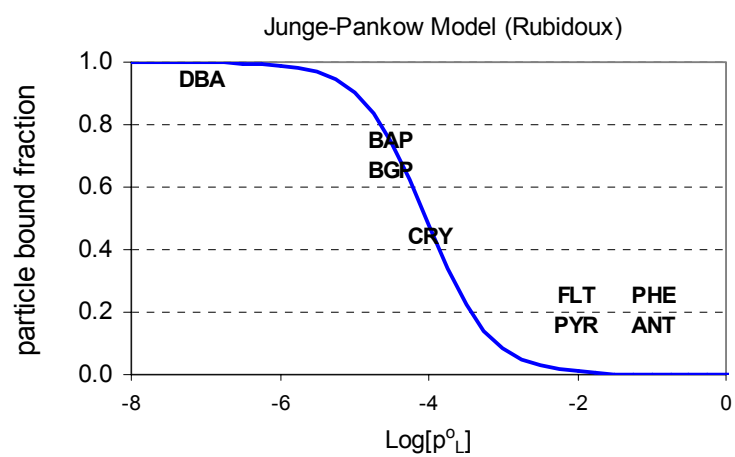


**Figure 9. Junge-Pankow Model calculated for Rubidoux vapor- and particle-phase PAH data.**

## 8. Characterization of PAH and PAH-Derivatives

### Background

The goal of our work is to characterize the polycyclic aromatic hydrocarbons (PAHs) and PAH-derivatives present at sites chosen to represent source sites or downwind receptor sites and to investigate the atmospheric chemistry occurring at these sites during different seasons. Of particular interest are nitro-PAH and nitro-polycyclic aromatic compounds (nitro-PAC) since these compounds are potent mutagens and have been observed as products of gas-phase atmospheric reactions of PAHs. During this reporting period ambient sampling was conducted at three monitoring sites, Los Angeles (urban site), and Riverside and Crestline (downwind receptor sites).

### Experimental section

Four time intervals per day were sampled for one week at Los Angeles (12-16 August 2002) and Riverside (26-30 August 2002). The daytime samples were 3.5 hours (morning 7am-10:30am, midday 11am-2:30pm and evening 3pm-6:30pm) and the nighttime sample was 11.5 hours (7pm-6:30pm). At Crestline, only 11.5 hours nighttime samples were taken and sampling was conducted only when O<sub>3</sub> levels were high.

The sampling sites were equipped with the following instrumentation: a Tenax solid adsorbent sampler, operating at 200 cm<sup>3</sup> min<sup>-1</sup> for the daytime samples and at 100 cm<sup>3</sup> min<sup>-1</sup> for the nighttime samples; a high-volume sampler with 2 polyurethane foam plugs (PUFs) located in series beneath a Teflon-impregnated glass fiber (TIGF) filter (20 cm × 25 cm) operated at ~0.6 m<sup>3</sup> min<sup>-1</sup>. Volatile compounds are collected onto Tenax solid adsorbent cartridges. The semi-volatile compounds are collected onto polyurethane foam plugs (PUFs), and the particles are collected onto filters. The Tenax samples are thermally desorbed onto a column of a GC-MS. PUFs and filters are soxhlet extracted in dichloromethane (DCM) for about 10 hours. Each PUF is spiked with a solution of nitronaphthalene-d<sub>7</sub>, phenanthrene-d<sub>10</sub>, fluoranthene-d<sub>10</sub> and pyrene-d<sub>10</sub>. The extracts of each time period were combined for analysis. The extracts were concentrated by rotary evaporation under vacuum, filtered through 0.45 μm Acrodiscs and fractionated by high performance liquid chromatography (HPLC). Nine fractions of increasing polarity were collected. Fractions 2-3 contain the PAHs, fraction 4 contains the nitro-PAHs and the polar compounds such as the oxygenated PAHs are collected in fractions 5-7. The fractions are analyzed by GC-MS for identification of compounds.

## Results and Discussion

To date we have analyzed the tenax samples and the semi-volatile nitro-PAHs collected on the PUFs. We are particularly interested in the methyl-, and dimethyl-nitronaphthalenes. All 14 isomers of methylnitronaphthalenes (MNN) and about 30 of the possible 55 isomers of the dimethylnitronaphthalenes (DMNN) have been identified in HPLC fraction 4 of the ambient samples.

The relative isomer abundance of the daytime samples and the nighttime sample differed, especially for the samples collected at Riverside. The differences in the MNN profiles for the daytime samples and the nighttime samples are shown in Figures 1 and 2 for Los Angeles and Riverside, respectively. The differences in MNN profiles are due to differences in atmospheric chemistry. At nighttime, MNN are formed by  $\text{NO}_3$  radical chemistry and lead mainly to the formation of 2-methyl-4-nitronaphthalene (2M4NN). During daytime, MNN are formed by OH radical chemistry, forming mainly 1M6NN and 1M5NN. Since the daytime and nighttime MNN profiles are very similar at Los Angeles, there is little evidence for the occurrence of nighttime  $\text{NO}_3$  chemistry. In order to have  $\text{NO}_3$  chemistry,  $\text{NO}_2$  and  $\text{O}_3$  need to be present. However, fresh emissions of NO in an urban area could rapidly react with any  $\text{NO}_3$  radical formed. At Riverside, there is some evidence of nighttime  $\text{NO}_3$  chemistry, characterized by a higher concentration of the 2M4NN in the nighttime sample versus the daytime sample. However the high concentrations of 1M6NN and 1M5NN in the nighttime sample indicate that the nitro-PAHs formed by OH radical chemistry during the day remain in the atmosphere and are sampled at night.

Differences in the DMNN profiles for the daytime and nighttime samples were also observed. Under separate funding, chamber studies to identify the origins of the DMNNs are continuing. Future work will include data analysis of the tenax samples and extraction and analysis of the filter samples taken in Riverside and Los Angeles.

Figure 1: Mass chromatograms for the molecular ion ( $m/z$  187) of the methylnitronaphthalenes from the GC/MS analysis of daytime and nighttime samples from Los Angeles

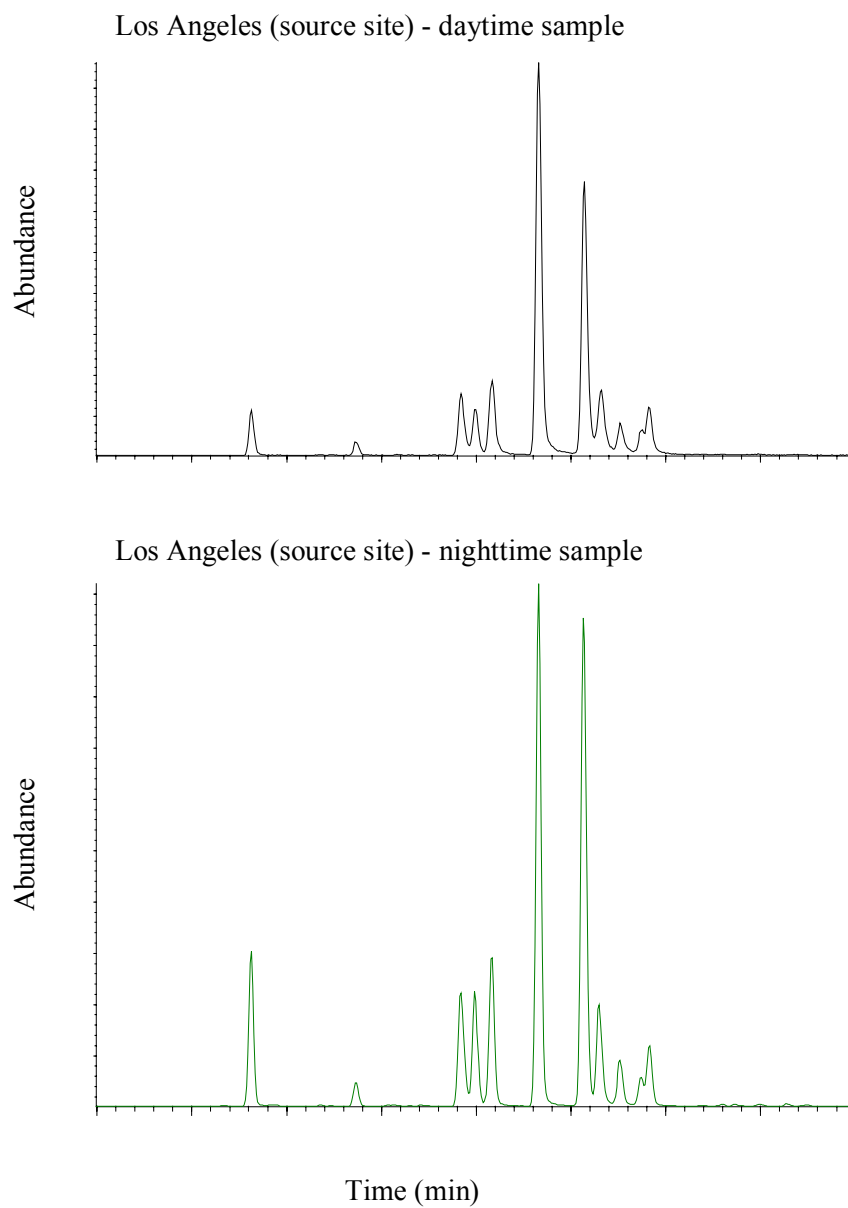
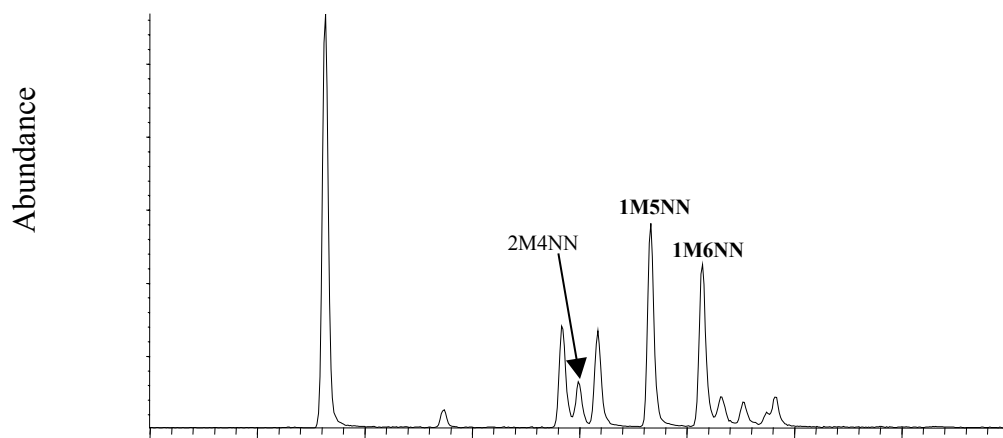
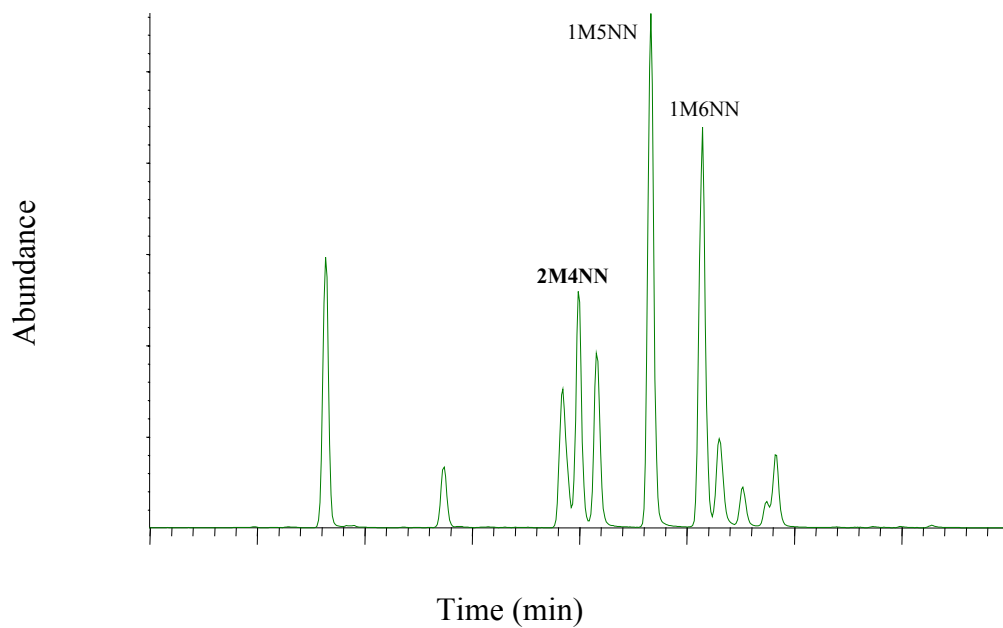


Figure 2: Mass chromatograms for the molecular ion ( $m/z$  187) of the methylnitronaphthalenes from the GC/MS analysis of daytime and nighttime samples from Riverside

Riverside - downwind receptor site (daytime sample)



Riverside - downwind receptor site (nighttime sample)



## **9. Field Evaluation Of The Differential Teom Monitor In Claremont, California**

### **I. Introduction**

Particulate matter (PM) in ambient air is composed of many chemical species of varying vapor pressures. A direct mass measurement of PM mass on filters is the basis of regulatory PM reference methods. The loss of semi-volatile PM mass collected on filters and filter sampling artifacts can produce non-quantifiable biases in reference method measurements depending on the thermodynamic history of the filter, therefore a reference method cannot be considered a scientific reference standard. Two prototype Differential TEOM<sup>®</sup> monitors (Patashnick, et al., 2001), has been tested in a major field study sponsored by the U.S. EPA. For nearly one year the Differential TEOM monitors have been co-located with integrated and semi-continuous mass monitors in the PIU at the Southern California Supersite location in Claremont, CA - a site high in semi-volatile organic- and Nitrate-associated PM. This location and research facility was ideal for the field evaluation and testing the ability of the Differential TEOM monitor to perform in a challenging environment. The field evaluation was conducted, as a collaboration between the PIU and the manufacturer, Rupprecht & Patashnick, co., Inc., as there is a strong suggestion that a practical reference standard for PM mass is possible with this instrument, and also to support a major emphasis of the Southern California Supersite: to characterize and develop novel state-of-the-art particulate monitors. This report is excerpted from the manuscript that is slated for submission to the journal *Aerosol Science & Technology*, as part of a Supersite special issue (Jaques, et al., 2002).

## **II. Test Equipment**

### **A. Differential TEOM**

#### **1. Theory of Operation**

The Differential TEOM monitor concept, based on the direct mass reading and real-time capability of the well-established TEOM mass monitor (Patashnick et al, 1991). The Differential TEOM monitors used during this study were refined from the concept described previously. Instead of a matched pair of TEOM sensors, the system used during this study operated as a self-referencing mass monitor, utilizing a single mass sensor instead of the two mass sensors described in the paper. The system used in this study is depicted in Figure 1. As presented in the figure, the system consists of a size-selective inlet, in this case a PM-10 inlet followed by a PM-2.5 sharp-cut cyclone, and then a Nafion<sup>®</sup> dryer. Downstream from the Nafion dryer and ahead of the TEOM sensor is an electrostatic precipitator (ESP). The ESP selectively removes aerosol from the sample stream at predetermined time periods. The ESP was alternately switched on and off, in this case for equal time periods,  $\Delta t$ . Frequency data was collected from the TEOM sensors on a continuous basis. (The measured frequency can be converted to a measured mass through a simple spring mass approach and is described in detail by Patashnick and Rupprecht (1991).)

It is possible to write a somewhat simplified expression for the "effective" amount of mass,  $M_{\text{eff}}$ , measured by the mass sensor during the two time periods,  $\Delta t_n$  when the ESP is turned off and alternately when the ESP is energized. The effective mass for each period is the mass that is calculated from the frequency of the TEOM sensor including all sources that affect the frequency during the given time period. For the periods when the ESP is turned off, the subscript A is used, and for the periods when the ESP was energized, the subscript B is used.

In that case for the periods when the ESP was turned off:

$$M_{\text{Aeff}} = M_{\text{pnv}} + M_{\text{pv}} - \forall M_{\text{pv}} \forall M_{\text{filt art.}} \forall M_{\text{eff)T, etc.}} \quad (1)$$

Where:

$M_{\text{Aeff}}$  = Effective mass reported during the time  $\Delta t_n$

$M_{\text{pnv}}$  = non-volatile component of particle mass collected during the time interval

$M_{\text{pv}}$  = volatile component of particle mass collected during the time interval

$\forall M_{\text{pv}}$  = fraction of volatile mass that vaporizes during the time interval

$M_{\text{filt art.}}$  = mass gain or loss due to filter artifacts during the time interval

$M_{\text{eff)T, etc.}}$  = effective mass equivalent of frequency change due to temperature and/or other sensor sensitivities during the time interval

For the periods when the ESP is energized, particles are not collected on the filter, but are removed from the sample stream inside of the ESP.  $M_{\text{pnv}}$  and  $M_{\text{pv}}$  are absent from this equation as this material is removed from the sample stream and retained in the ESP. Volatilization of previously collected particles and any adsorption of gaseous species in the sample stream continues:

$$M_{\text{Beff}} = - \forall M_{\text{pv}} \forall M_{\text{filt art}} \forall M_{\text{eff)T, etc.}} \quad (2)$$

Comparing two adjacent time periods yields the effective mass concentration of the system over two switching periods of the ESP:

$$M_{\text{eff}} = M_{\text{Aeff}} - M_{\text{Beff}} = M_{\text{pnv}} + M_{\text{pv}} \quad (3)$$

The technique works due to the referencing aspect of the TEOM sensors. The switching time of the ESP must be chosen to be less than the time for changes to occur in the ambient particle concentration. In addition, the chosen time interval must be less than the time it takes for a volatile species of interest on the particles to vaporize, however by averaging a number of sequential switch periods reduces the impact of short-term changes in the ambient conditions. Clearly, the system approaches the most accurate representation of particle mass as it exists in its undisturbed state in the atmosphere as  $\Delta t$  approaches zero. There are practical limits to the minimum time for switching the ESP on and off.

An important point to note is that the Differential TEOM system eliminates the problems



associated with other particle measurement techniques (including manual filter systems) especially in its handling of volatile material, as a result of the strongest feature of TEOM instrumentation: direct mass measurement in real time.

The mass concentrations during each switch segment were calculated by obtaining the least squares fit of the frequency data during each ESP switch interval and converting the computed slope,  $df/dt$ , to mass change,  $dm/dt$ , through the calibrated TEOM detectors. Dividing by the flow rate yields the effective mass concentration for each detector at each interval.

## **2. Interpretation of Data**

Unlike a standard TEOM monitor which collects sample and reports mass concentration continuously, the Differential TEOM monitor is only collecting mass on the TEOM sample filter during half of the operating time of the monitor. During the other half of the operation, the ESP is energized and only the effects of the sampled gases and any evaporation of previously collected sample are observed by the TEOM sample filter. As described above in the theory of operation, this allows the system to self-correct and determines the amount of material collected by the monitor at the time of collection. FRM samples on the other hand, are strictly dependent on the sample and sample artifacts that are collected during the history of the sample. Figure 2 assists in elucidating this critical aspect. There are three lines presented on the figure, the final reported ambient mass concentration, the mass concentration determined when the ESP was energized, and finally the mass concentration when the ESP is turned off. By subtracting the mass concentration during periods when the ESP is energized from the mass concentration when the ESP is turned off results in a reportable ambient mass concentration. The figure is also divided into two sections. The left side of the figure depicts a period where there is primarily evaporation of previously collected material from the TEOM sample filter during the periods when the ESP is energized, and the right side of the figure depicts similar data when there is adsorption onto the TEOM sample filter. The figure represents a composite of data collected at different times and locations, but was joined onto a common graph only to illustrate how the data collected from the Differential TEOM is interpreted for analysis. The graph is not meant to represent any specific event or sample location.

### **a. ESP energized sampling periods**

During the periods when the ESP is energized, no collection of "particles" is occurring. That is, all of the non-volatile and semi-volatile particle matter is being captured in the ESP and does not reach the sample filter. However, there may still be events occurring that are measured by the sample filter in the Differential TEOM monitor. These can include evaporation of the previously collected material, adsorption of gas phase species onto the collected sample or sample filter, or mass changes caused by chemical reactions on the filter surface.

The left side of the figure shows the results when there was the evaporation of the previously collected material. The mass concentration for the sampling segments when the ESP was energized were negative, representing a net loss from the sample filter during these periods.

There may still be adsorption or other non-particle increases in the sample mass, but the overall effect of all sample and filter artifacts is to create a net negative mass concentration. In the right side of the figure, the reported mass concentration for the ESP energized segments is positive. This generally results from gas adsorption onto the sample filter and previously collected material.

In general, the greater the value deviates from zero, the greater amount of activity on the sample filter. Just because the mass concentration is zero when the ESP is energized does not mean that there is no volatile components either being evaporated or adsorbed, just that the relative activity is balanced resulting in a net change of zero.

#### **b. ESP de-energized sampling periods**

During the periods when the ESP is turned off, or de-energized, the Differential TEOM monitor collects sample as a standard TEOM monitor. During this period, non-volatile and semi-volatile particles are collected on the sample filter, increasing the reported mass on the sample filter. At the same time, the identical behavior as observed when the ESP was energized is also occurring. That is previously collected semi-volatile material may evaporate, reducing the mass on the filter, and gas phase species may adsorb onto the sample filter or material collected on the sample filter. As far as the monitor is concerned, there is no real difference in operation between the different operational segments. The TEOM sensor is acting as a near real-time mass monitor of the overall mass of the sample filter.

Apart from the collection of non-volatile and semi-volatile material on the sample filter during this period, all other effects and artifacts are also occurring at the same rate as that happening during the periods when the ESP is energized. If there is evaporation of previously collected material, identical evaporation is happening during the adjacent segments when the ESP is not energized since the wetted surfaces are the same regardless of whether the ESP is energized or not.

#### **c. Reported mass concentrations**

The third line presented in the figure is the reported mass concentration. This is the effective mass concentration measured by the instrument and is the result of subtracting the concentration for the periods when the ESP is energized from the concentration reported when the ESP is turned off. When there is evaporation from the TEOM sample figure, as illustrated in the left side of the figure, the resultant ambient mass concentration is greater than the concentration obtained during normal sampling. When there is adsorption onto the TEOM sample filter, the resultant mass concentration is lower than the normal sampling concentration. Since the artifacts, evaporation or adsorption, for example, are always occurring, the net result is that the reported mass concentration will never be less than zero. As the artifacts increase and the amount of collected material decreases, the final result may approach zero. This is illustrated in the results presented on the right side of the figure. There is a short segment where the data

when the ESP was turned off and when the ESP was energized are almost identical and the resulting reported mass concentration is nearly zero.

## **B. PIU Integrated and Semi continuous Monitors for comparison**

To reference the Differential TEOM measurements, 24 hour time-integrated filter-based PM-2.5 monitors were co-located at the PIU in Claremont: 1) a MOUDI (Model 110; MSP Corp., MN); and a Partisol (Model 2025; Rupprecht and Patashnick Co., NY); and to evaluate semi-volatile losses of filter-based ammonium nitrate, an annular denuder (HEADS) was used. 24-hour integrated time series plots and correlations are used to compare with the Differential TEOM. A more complete description and discussion of these integrated mass and chemical measurements are in Section 3 of this report.

## **III. Results and Discussion**

### **A. Instrument Precision**

In Figure 3 paired identical differential TEOM monitors are compared using 24-hour time-integrated data over a 7-month period at Claremont. Over all, the precision of the two instruments is very good, nearly 5%, as indicated by the Coefficient of Determination ( $R = 0.946$ ). The slope of 0.999 also strongly supports that there is no bias between these two instruments in this application.

### **B. Instrument Intercomparison**

#### **1. FRM Comparison and MOUDI Comparison**

Figure 4 presents a pair of scatter plots referencing the Differential TEOM monitor and Partisol to 24-hour integrated measurements by the MOUDI. For discussion and comparison purposes, the MOUDI is used as the reference, herein, as it has been found to be more comparable to a continuous monitor that measures the volatile component of Nitrate predominantly found in this region of Los Angeles (Fine, et al., 2002). These co-located results are highly correlated ( $R^2 = 0.87$  and  $0.83$ , respectively). However, the Partisol underestimates the MOUDI measured mass by about 17%, while the Differential TEOM is highly comparable and higher than the MOUDI by about 7%. Although 12 data pairs are presented herein, upon the final validation of Differential TEOM monitor data, the N will increase substantially, thus potentially improving the correlation and significance of these results. The results obtained using the Differential

TEOM monitor are expected to be greater than that of the MOUDI and Partisol, assuming that the particulate air sample was dominant in semi-volatile, rather than adsorbed material. Additionally, by using either the MOUDI or Partisol as a reference, these results suggest that the Differential TEOM monitor may account for the potentially desorbed semi-volatile compounds associated with PM-2.5. However, being higher, may also suggest that it gains mass by adsorption, although as discussed in Section 2 above, adsorption of gases onto the TEOM sample filter are subtracted out of the final mass concentration measurements.

### **C. Differential TEOM Monitor/Nitrate Comparisons**

24-hour time-integrated PM<sub>2.5</sub> mass measurements collected using the Differential TEOM monitor, and the MOUDI are paired with NH<sub>4</sub>NO<sub>3</sub> measurements made by both the MOUDI and Harvard Annular Denuder (HEADS) for the full course of this one-year study at Claremont (Figure 5). The Differential TEOM monitor data is limited to 12 points, until quality assurance of the data is completed. For this limited data, the Differential TEOM monitor results track the results collected by the MOUDI, and on 9 of 12 occasions are generally greater than the MOUDI - as much as 9 ug/m<sup>3</sup> (February 15). This suggests that mass evaporation from the MOUDI filter dominates that imposed by adsorption for a majority of the time. NH<sub>4</sub>NO<sub>3</sub> measurements demonstrate not only that the HEADS and MOUDI track the Differential TEOM monitor and MOUDI mass results, but that the HEADS is always greater. Also, for high mass days, NH<sub>4</sub>NO<sub>3</sub> tends to be the dominant compound attributable to the mass. These factors suggest that the difference in mass between the Differential TEOM monitor mass results and the MOUDI mass results is largely due to Nitrate losses from the MOUDI. The difference between the Differential TEOM monitor and MOUDI mass results are correlated against the difference of Nitrate between the HEADS and MOUDI, as measured on the same MOUDI filters. For the 10-paired differences, the “Mass Loss” has a relatively high correlation with that of “Nitrate Loss” ( $R^2 = 0.645$ ). Also, 7 of the 10 pairs are greater in “Mass Loss” (between 0.4 and 8.8 ug/M<sup>3</sup>), and between 1.2 and 4.2 ug/M<sup>3</sup> for “Nitrate Loss”. These results strongly support that much of the mass lost on the Differential TEOM filter is due to Nitrate evaporation. Albeit, this is only revealed in the MOUDI being lower, while the Differential system subtracts this out. The 3 paired-data that result in negative differences in “Mass Loss” (between 2.1 and 4.8 ug/m<sup>3</sup>) indicate that more mass was gained by the MOUDI than lost. For these occasions, Nitrate measured by the HEADS is greater than that for the MOUDI, suggesting that the mass loss is not dominated by the adsorption of vapor phase Nitrate onto the substrate, but likely due to the adsorption of vapor phase organic compounds. These paired measurements cannot quantitatively determine the amount of evaporation, or adsorption, in part because of the dynamics of these co-existing processes, especially when integrated over 24-hours. The relative amount of adsorption may be qualitatively inferred by observing the semi-continuous measurements made by the Differential TEOM monitors shown in the representative figure on the interpretation of the Differential TEOM monitor results (Figure 2).

## Summary and Conclusions

Two Differential TEOM monitors were field tested and characterized at the Claremont Los Angeles Supersite location for nearly one year. 24-hour integrated measurements of this semi-continuous monitor have been compared to the PM mass and Nitrate mass of other filter-based systems that ran concurrently. Although there is no true reference for particulate mass, in general the Differential TEOM monitor compares well with these other methods and suggests that the Differential TEOM monitor could be used as a new reference standard for particulate mass. Comparisons of two co-located Differential TEOM monitors demonstrates high precision, suggesting a reliable method. Future analysis of other semi-continuous mass, Nitrate, and Organic Carbon can be conducted to more closely evaluate the dynamic chemical processes that occur on the filter over time.

## References

Patashnick, H., Rupprecht, G., Ambs, J. L., and Meyer, M. B., "An Advanced TEOM<sup>®</sup> System for Exact Particulate Matter Mass Determination in Ambient Air", presented at the 93 Air and Waste Management Association meeting.

Patashnick, H.; Rupprecht, E. *J. Air Waste Management Association* 1991, 41, 1079-1083

Shen S; Zhu Y, Jaques PA; and Sioutas C. Evaluation of the SMPS-APS system as a Continuous Monitor for PM<sub>2.5</sub> and PM<sub>10</sub>. Accepted *Atmospheric Environment*, February 2002.

Fine PM; Jaques PA; Hering SV; and Sioutas C. Performance Evaluation and Use of a Continuous Monitor for Measurement Size-Fractionated PM<sub>2.5</sub> Particulate Nitrate. Submitted for Publication to *Aerosol Science and Technology*, April 2002.

Jaques, PA; Ambs, JL; Grant, WL.; Sioutas, C. Field Evaluation Of The Differential Teom<sup>®</sup> Monitor By Comparison With Semi-continuous And Integrated Ambient Particulate Mass And Nitrate In Claremont, California. *Aerosol Science and Technology*, October 2002; to be submitted as part of a special Supersite issue.

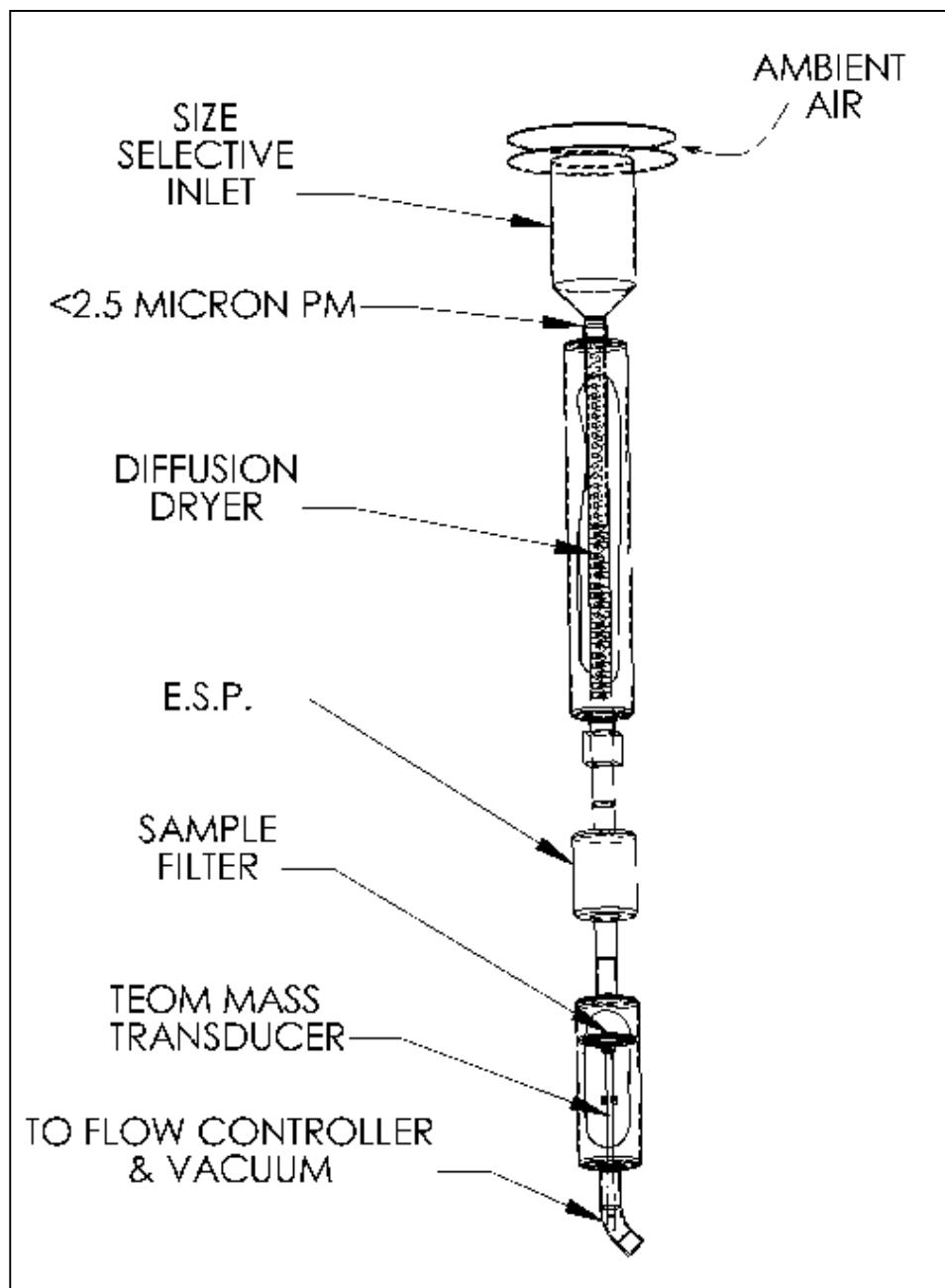


Figure 1. Schematic of the prototype Differential ESP TEOM, noting a linear sample train, modified from the earlier version with parallel ESP's used to minimize large particle losses.

# **Differential TEOM Data Illustrating Sample Evaporation and Adsorption** **Running average of hourly data for a Typical Day**

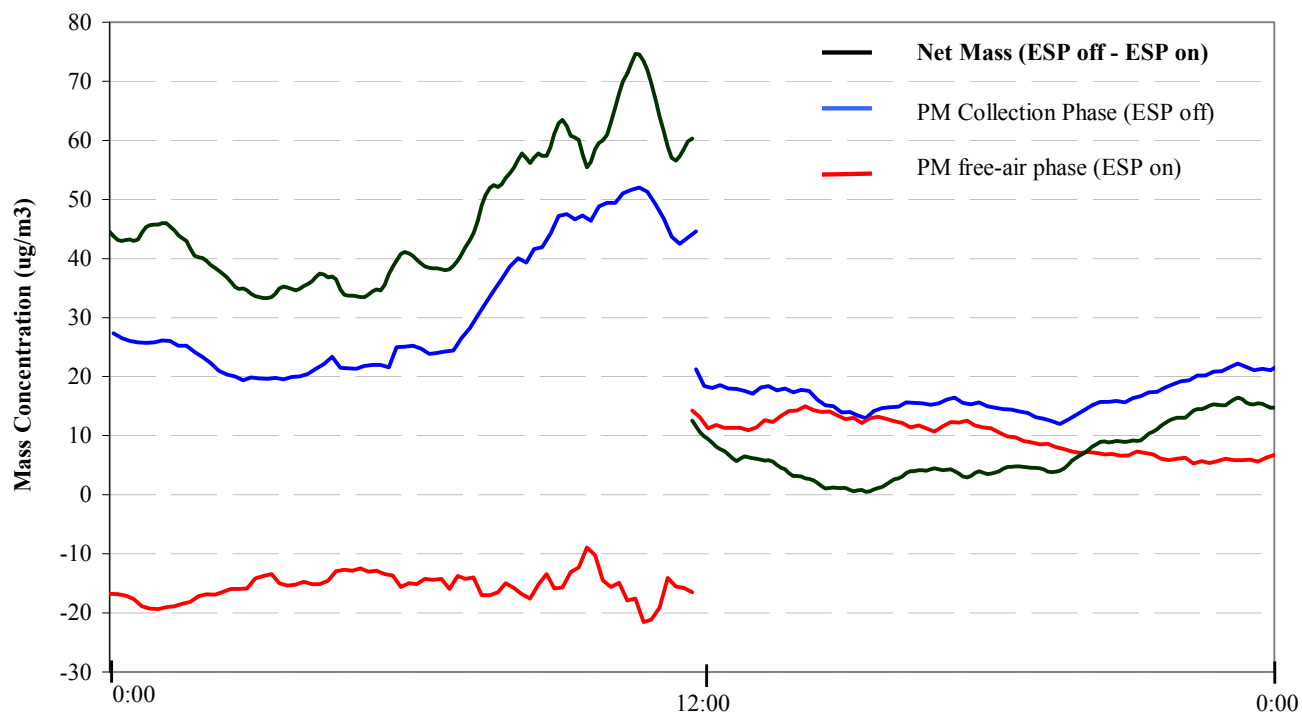
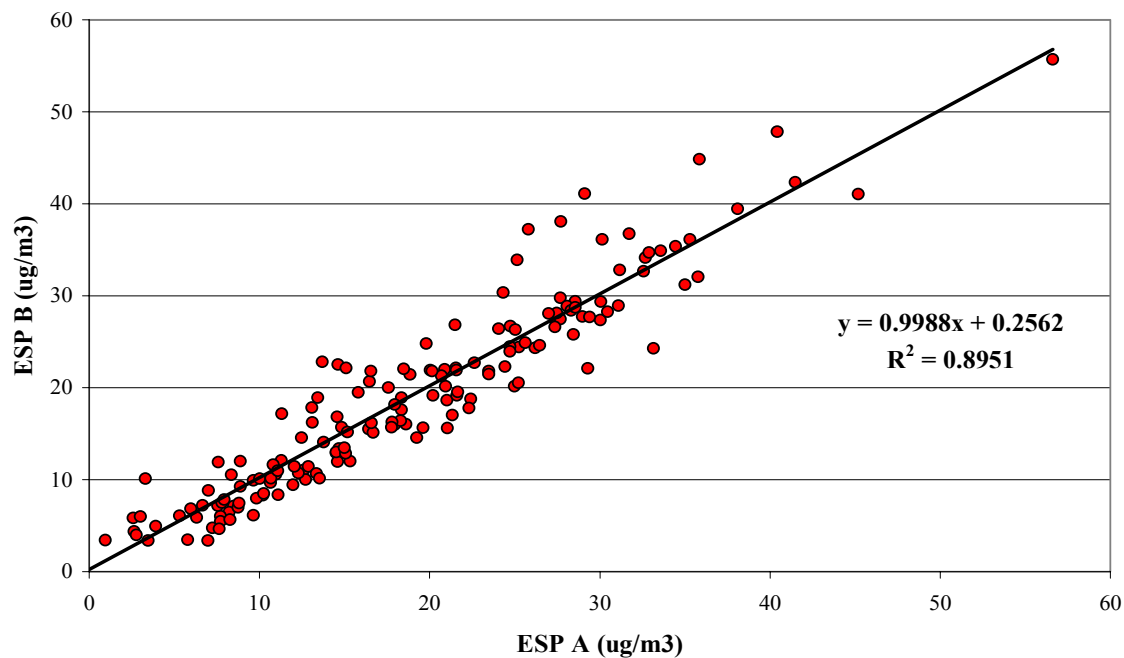


Figure 2. Time series composite of typical hourly data used for the interpretation of gas phase and particle laden air. Each segment of the figure represents approximately 12 hours of data collection.

**Paired Differential TEOM's 24-hour Integrated measurements  
Claremont, CA; Feb 2002 - Aug 2002**



**Figure 3. Scatter plot of 2 identical Differential TEOM's, presenting co-located 24 hour measurements in PIU at Claremont, CA.**

**Differential ESP TEOM & Partisol vs MOUDI  
Claremont, Sept 2001 - August 2002**

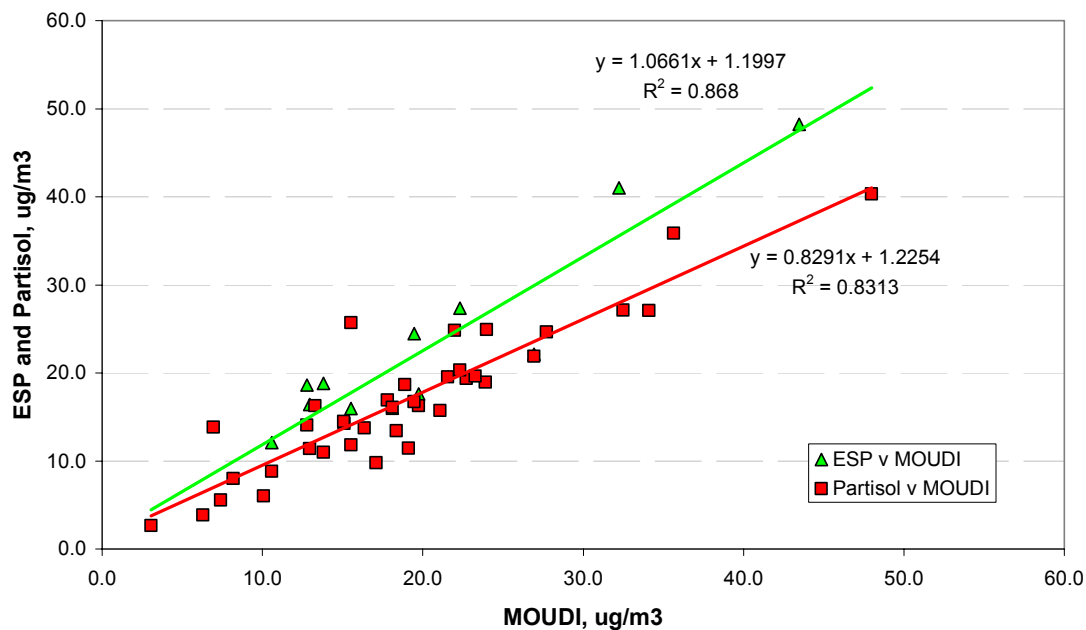


**Figure 4. Scatter plot of ESP and Partisol to MOUDI for one year period.**



**24 Hour PM2.5 Mass by Integrated and Continuous Monitors  
Claremont, September 2001 to August 2002**

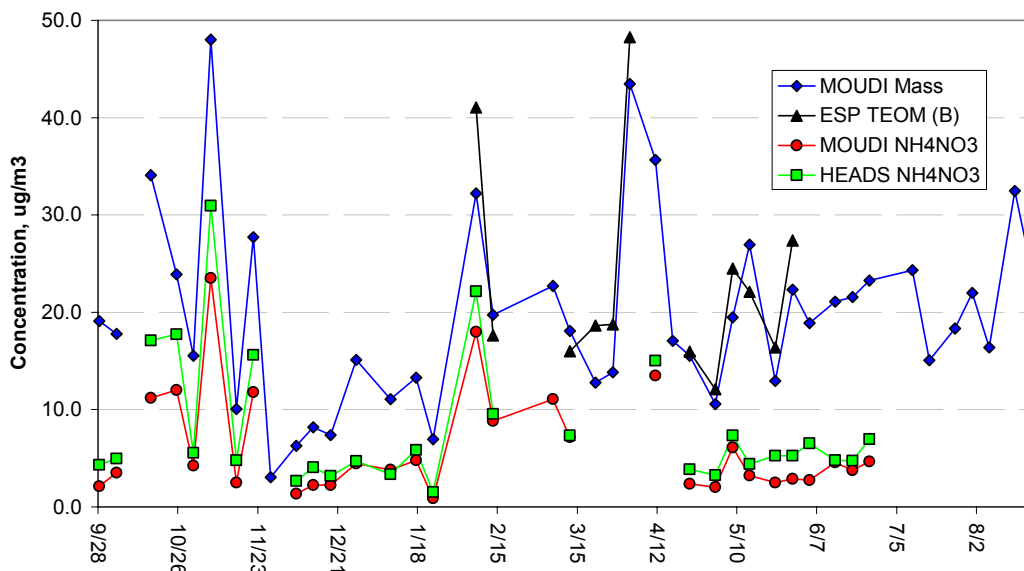


**Figure 5. Time series plot of MOUDI and ESP PM2.5, and MOUDI and HEADS NH4NO3 for one year.**

**Fine Mass Difference between the ESP and MOUDI vs  
Fine Nitrate by the HEADS and MOUDI**

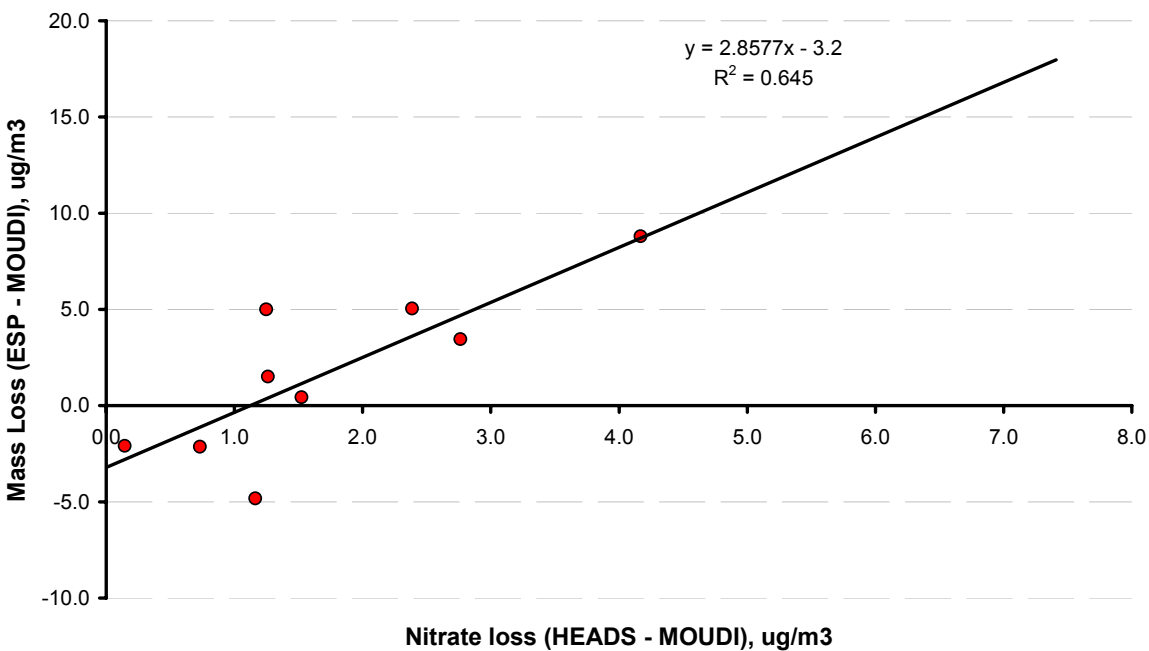


**Figure 6. Scatter plot presenting the relationship of mass and Nitrate lost by MOUDI with ESP and HEADS as reference.**

## 10. Automated, Size- and Time-Resolved Measurements of Particulate Carbon and Nitrate

From January to September 2002, we have simultaneous, size-resolved data on PM<sub>2.5</sub> nitrate and carbon concentrations at the Claremont site. Measurements are made for both species using our cascaded integrated collection and vaporization systems (ICVS) as described in previous reports. Both nitrate and carbon measurements will continue at the next site at USC, with data collection scheduled to begin September 18, 2002.

We experienced a significant period of malfunction in June due to CO<sub>2</sub> content in a tank of air for the carbon monitor carrier gas. Dry (CO<sub>2</sub> free) air was substituted once the error was discovered.

The humidity control system from the Carbon ICVS was removed for laboratory testing to improve humidity stability. The humidity for Cells A and B was recently observed to fluctuate regularly between 62 and 66% RH several times per minute (target humidity is 65% RH). The electronic controller will be retuned to limit this fluctuation and the humidity system will be reinstalled during setup at the USC site.

Recent data are included below. In Figure 1, Carbon data show a clear diurnal trend in mass on Cell C (0.1-0.5  $\mu$ m), peaking between 1500-1700. Increased vehicle exhaust emissions during evening rush hour could account for this daily rise in small primary carbonaceous particles. The larger two size fractions are not as plainly periodic. Figure 2 shows representative nitrate data during the recent period.

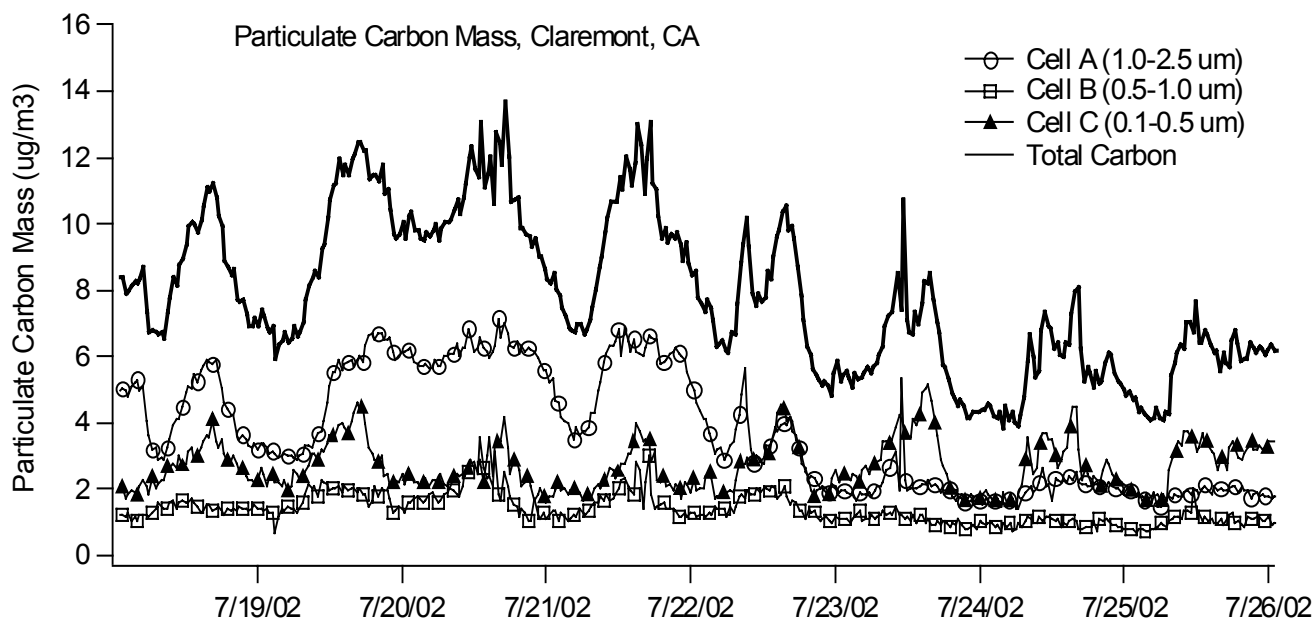


**Figure 1. Particulate carbon mass by size fraction, Claremont, California.**

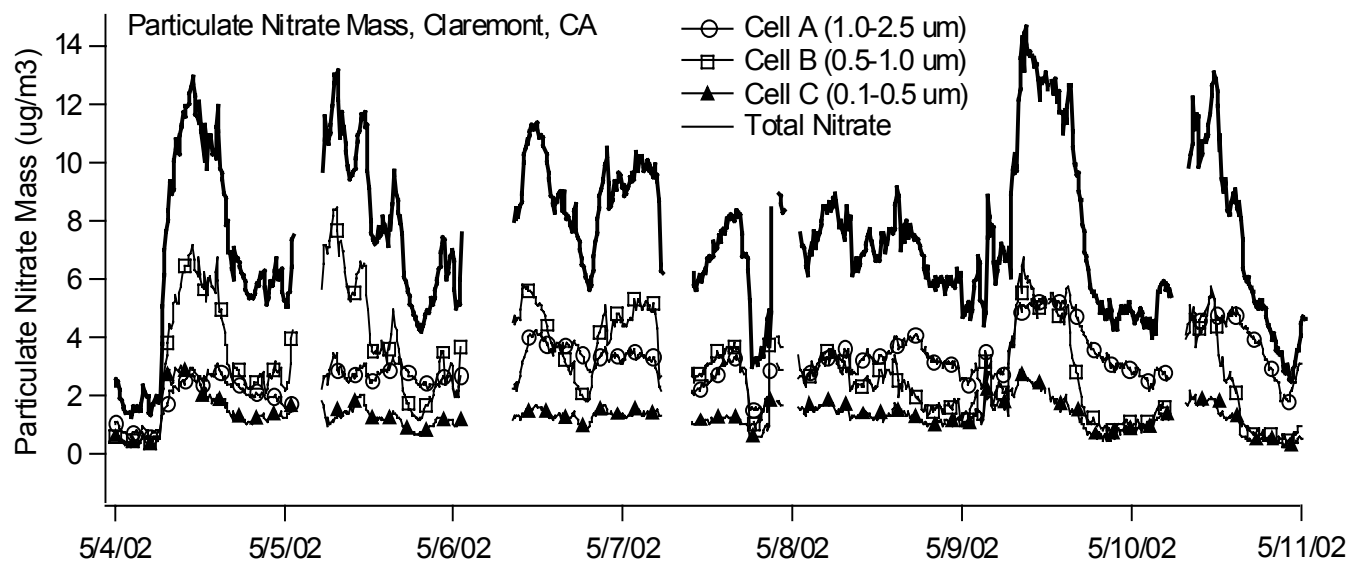


**Figure 2. Particulate nitrate mass by size fraction, Claremont, California.**

## 11. Ultrafine Particles near Major Freeways

Recent toxicology studies have demonstrated that atmospheric ultrafine particles are responsible for some of the adverse health effects. Motor vehicle emissions usually constitute the most significant source of ultrafine particles (diameter  $< 0.1 \mu\text{m}$ ) in an urban environment, yet, little is known about the concentration and size distribution of ultrafine particles in the vicinity of major highways. In the present study, systematic measurements of the concentration and size distribution of ultrafine particles in the vicinity of Interstate 405 (mostly gasoline traffic) and Interstate 710 (heavy-duty diesel traffic) in Los Angeles were carried out during the summer of 2001 and the winter 2002. Two papers have been published based on these studies:

- (1) Yifang Zhu, William C. Hinds, Seongheon Kim and Constantinos Sioutas, 2002, Concentration and Size Distribution of Ultrafine Particles near a Major Highway. JAWMA, 52: 1032-1042.
- (2) Yifang Zhu, William C. Hinds, Seongheon Kim, Si Shen and Constantinos Sioutas, 2002, Study of Ultrafine Particles near a Major Highway with Heavy-duty Diesel Traffic. Atmospheric Environment, 36: 4323-4345.

A third paper, comparing the seasonal differences of ultrafine particles in the vicinity of these two freeways has been submitted to Aerosol Science and Technology.

## **12. Data Management of LA Supersite**

### **Summary**

Major progresses during this quarter include: 1) submit SMPS data of Downey, Riverside, Rubidoux, and Claremont sites to NARSTO; 2) submit APS data of Downey, Riverside, and Rubidoux sites to Dr. Seung-Hoon Lee, an associate of Prof. Philip K. Hopke at Clarkson University, for an EPA extended project that agreed Baltimore Supersite to collect Supersite data and build relational databases; and 3) upgrade our data center website from FTP site to a web-based data-driven site in the coming near future.

### **Submission of SMPS data to NARSTO**

SMPS data of four sites submitted to NARSTO include:

- two Downey data sets from 12/08-12/10/2000 (EPA\_SS\_LA\_DWNY\_SMPS\_20001208\_20001210\_V1.csv) and from 12/13/2000 – 02/05/2001 (EPA\_SS\_LA\_DWNY\_SMPS\_20001213\_20010205\_V1.csv),
- one Riverside data set from 02/14/2001 – 06/05/2001 (EPA\_SS\_LA\_RVSD\_SMPS\_20010214\_20010605\_V1.csv),
- two Rubidoux data sets from 06/25/2001 – 08/22/2001 (EPA\_SS\_LA\_RBDX\_SMPS\_20010625\_20010822\_V1.csv) and from 08/22/2001 – 09/08/2001 (EPA\_SS\_LA\_RBDX\_SMPS\_20010822\_20010908\_V1.csv), and
- one Claremont data set from 09/17/2001-02/22/2002 (EPA\_SS\_LA\_CLMT\_SMPS\_20010917\_20020222\_V1.csv).

Table 1 shows sampling date, number of channels set for sampling particles, particle size ranges, and number of records by date/time.

### **Submission of APS data to Clarkson University**

Three APS data sets, which have been set to NARSTO, were sent to Dr. Seung-Hoon Lee at Clarkson University. This was an extended submission based on an e-mail from Dr. Paul A. Solomon, ORD Technical Lead, EPA's PM Supersites Program, on August 29, 2002. EPA has entered an agreement with the Baltimore Supersite to develop a relational database for the Supersite program. Two coordinated intensives that were held in July 2001 and January 2002 initiated a collection of Supersite data sets that will be useful to a wide variety of users. The rationale was to establish a common and easily accessible relational database and management system so that redundant efforts would be reduced to analyze integrated data sets from different sites. LA Supersite participates in this data submission program. We will continue to submit data sets to Clarkson University, whenever the data submitted to NARSTO have been officially approved. This is to assure that the data sets received by Clarkson University have the same quality as those published by NARSTO.

The three APS data sets sent to Clarkson University include:

- one Downey APS data set collected from 12/08/2000 – 02/05/2001  
(EPA\_SS\_LA\_DWNY\_APS\_20001208\_20010205\_V1.csv)
- one Rubidoux APS data set collected from 06/25/2001 – 09/08/2001  
(EPA\_SS\_LA\_RBDX\_APS\_20010625\_20010908\_V1.csv)
- one Riverside APS data set collected from 02/14/2001 – 06/05/2001  
(EPA\_SS\_LA\_RVSD\_APS\_20010214\_20010605\_V1.csv)

Table 2 shows sampling date, number of channels set for sampling particles, particle size ranges, and number of records by date/time.

### **Upgrading LA Supersite Database System**

LA Supersite has started to accumulate air pollution data sets, including air monitoring data from PIU, and in vitro and in vivo experiment data of SCPCS research projects that were attempted to relate toxicological endpoints to the former. The Data Center initiated to develop a web-based data-driven system, not only to store all data sets generated by LA Supersite, but also actively present the results and significance to potential users. Our long-term goals are to include Cal ARB data, Cal TRAN traffic count data, previously published data related air pollution in the LA basin, and air-pollution related health/toxicological information. This database system strives to become a resource center for air pollution health effects in Southern California. During this quarter, we started to upgrade a computer system to facilitate to reach our feature goals. Efforts include an increase in data storage capacity and design of a web-based data driven site.

**Table 1: Description of SMPS data sets Submitted to NARSTO**

<b>Data set</b>	<b>Sampling Dates</b>	<b>Particle Sizes (nm)</b>	<b># of Channels</b>	<b># of Records<sup>c</sup></b>
-----	-----	-----	-----	-----
	-			
<b>Downey –1</b>	<b>12/08/2000 –12/10/2000</b>	<b>14.9-673</b>	<b>54</b>	<b>232</b>
<b>Downey – 2</b>	<b>12/13/2000 – 02/05/2001</b>	<b>14.1 - 661</b>	<b>108<sup>a</sup></b>	<b>3721</b>
<b>Riverside</b>	<b>02/14/2001 – 06/05/2001</b>	<b>14.1 - 661</b>	<b>108<sup>a</sup></b>	<b>9245</b>
<b>Rubidoux – 1</b>	<b>06/25/2001 – 08/22/2001</b>	<b>21.7 - 429</b>	<b>84</b>	<b>5160</b>
<b>Rubidoux –2</b>	<b>08/22/2001 – 09/08/2001</b>	<b>14.1 - 638</b>	<b>107<sup>b</sup></b>	<b>1278</b>
<b>Claremont</b>	<b>09/17/2001 – 02/22/2002</b>	<b>14.1 - 638</b>	<b>107<sup>b</sup></b>	<b>12213</b>
-----	-----	-----	-----	-----
	-			

<sup>a</sup>Exclude three channel size with all values = 0. <sup>b</sup>Exclude four channel size with all values = 0. <sup>c</sup>A record consists of a series of variables, including particle concentration for a particular size, reported by SMPS for every 15 minutes.

**Table 2: Description of APS data sets Submitted to Clarkson University**

<b>Data set</b>	<b>Sampling Dates</b>	<b>Particle Sizes (µm)</b>	<b># of Channels</b>	<b># of Records<sup>b</sup></b>
-----	-----	-----	-----	-----
	--			
<b>Downey</b>	<b>12/08/2000 – 02/05/2001</b>	<b>&lt; 0.523 – 19.81</b>	<b>52</b>	<b>3053</b>
<b>Riverside</b>	<b>06/25/2001 – 09/08/2001</b>	<b>0.542 – 19.81</b>	<b>51<sup>a</sup></b>	<b>7736</b>
<b>Rubidoux</b>	<b>02/14/2001 – 06/05/2001</b>	<b>0.542 – 19.81</b>	<b>51<sup>a</sup></b>	<b>6179</b>
-----	-----	-----	-----	-----
	--			

<sup>a</sup>Exclude one channel size < 0.523. <sup>b</sup>A record consists of a series of variables, including particle concentration for a particular size, reported by APS for every 15 minutes.